

General Disclaimer

One or more of the Following Statements may affect this Document

- This document has been reproduced from the best copy furnished by the organizational source. It is being released in the interest of making available as much information as possible.
- This document may contain data, which exceeds the sheet parameters. It was furnished in this condition by the organizational source and is the best copy available.
- This document may contain tone-on-tone or color graphs, charts and/or pictures, which have been reproduced in black and white.
- This document is paginated as submitted by the original source.
- Portions of this document are not fully legible due to the historical nature of some of the material. However, it is the best reproduction available from the original submission.

JPL PUBLICATION 83-49



Evaluation of Aperture Cover Tank Vent Nozzles for the IRAS Spacecraft

Robert Richter

(NASA-CR-173101) EVALUATION OF APERTURE
COVER TANK VENT NOZZLES FOR THE IRAS
SPACECRAFT (Jet Propulsion Lab.) 45 p
HC A03/MF A01

N83-35006

CSCL 22B

G3/18 Unclas
42166

September 1, 1983



National Aeronautics and
Space Administration

Jet Propulsion Laboratory
California Institute of Technology
Pasadena, California

JPL PUBLICATION 83-49

Evaluation of Aperture Cover Tank Vent Nozzles for the IRAS Spacecraft

Robert Richter

September 1, 1983



**National Aeronautics and
Space Administration**

**Jet Propulsion Laboratory
California Institute of Technology
Pasadena, California**

The research described in this publication was carried out by the Jet Propulsion Laboratory, California Institute of Technology, under contract with the National Aeronautics and Space Administration.

Reference to any specific commercial product, process, or service by trade name or manufacturer does not necessarily constitute an endorsement by the United States Government or the Jet Propulsion Laboratory, California Institute of Technology.

FOREWORD

The work described in this report was performed in support of the Infrared Radiation Astronomical Satellite (IRAS) program. A. Giandominico and C. S. Guernsey, both members of the Jet Propulsion Laboratory, performed the testing of the nozzles, which were furnished by Ball Brothers, Inc., Boulder, CO., on the Micropound Extendable Range Thrust Stand (MERTS) at the RCA Corporation facility in New Jersey.

The effort described is an independent approach of the evaluation of the aperture cover tank nozzles for the IRAS spacecraft. It uses the raw test data of the flow tests of the five nozzles furnished by Ball Brothers, Inc. and the strip chart recordings generated during the testing of the nozzles on the MERTS thrust stand. The same test data obtained with the MERTS device have been employed in another independent evaluation by C. S. Guernsey.

At the time of publication of this report, the IRAS spacecraft has been in orbit for several months. The attitude of the spacecraft has been maintained stably.

TABLE OF CONTENTS

Section	Page
1. INTRODUCTION	1
2. DETERMINATION OF INFLUENCE COEFFICIENTS	2
2.1 ACT Nozzles	2
2.2 Basic Thermodynamic and Fluid Dynamic Relations	2
2.3 Effect of Boundary Layer on Total Thrust	3
2.4 Influence Coefficients	3
2.4.1 Coordinates and Coordinate System of IRAS Spacecraft	3
2.4.2 Torques Around the Three Major Spacecraft Axes	8
3. EXPERIMENTAL EVALUATION OF ACT NOZZLES	15
3.1 General Approach	15
3.2 Nozzle Evaluation by Sonic Flow Measurement	15
3.3 Testing of ACT Nozzles on MERTS Thrust Measuring Stand	22
3.4 Estimate of Angular Deviation of Thrust Vector	30
4. CONCLUSIONS	34
REFERENCES	35
Appendix	
A CONVERSION OF SPHERICAL COORDINATE ANGLES TO CLOCK AND CONE ANGLES	A-1
B MERTS THRUST MEASURING DEVICE PRINCIPLE	B-1

LIST OF ILLUSTRATIONS

Figure	Page
1 ATC Nozzle Thrust Characteristic	4
2 Deviation from Ideal Thrust	5
3 Analytically Predicted Thrust Differential	6
4 IRAS Spacecraft Coordinate System	7
5 Upper Bound for Torque Around the X-Axis	11
6 Upper Bound for Torque Around the Y-Axis	12
7 Upper Bound for Torque Around the Z-Axis (ΔF and θ)	13
8 Upper Bound for Torque Around the Z-Axis ($\Delta F/F$ and θ)	14
9 ACT Nozzle Design	16
10 Nozzle Calibrations of ACT Vent Nozzles #64874-5	18
11 Calculated Thrust Mismatch Between Nozzle S/N001 and Nozzles S/N002 through S/N005	21
12 Repeatability of Calibration of Micropound Thrust Stand (MERTS)	23
13 Indicated Thrust Mismatch Between Nozzles S/N001 and S/N002	24
14 Thrust Mismatch Between Two Nozzles Due to Temperature Difference	26
15 Measured Thrust Mismatch Between Nozzle S/N001 and Nozzles S/N002 through S/N005	27
16 Indicated Thrust Mismatch Between Nozzles S/N004 and S/N003	28
17 Effect of Torque Direction on Indicated Torque	29
18 Possible Angular Thrust Vector Misalignment Combinations 32 for Measured Torque with Nozzle Pair S/N002 and S/N004	32
B-1 Geometrical Parameters of the MERTS Thrust Balance	B-1

LIST OF TABLES

Table	Page
1 Coordinates of the ACT Nozzles and the Center of Mass of the IRAS Spacecraft	3
2 Influence Coefficients of the Three Major Nozzle Parameters	9
3 Allowable Deviations for the Three Major Nozzle Parameters	10
4 Sonic Flow Measurements of Nozzles #64874-5	17

ABSTRACT

The influence of coefficients for the three axes of the Infrared Astronomical Satellite (IRAS) were established to determine the maximum allowable thrust difference between the two vent nozzles of the Aperture Cover Tank (ACT) Low Thrust Vent system and their maximum misalignment. Test data generated by flow and torque measurements permitted the selection of two nozzles whose thrust differential was within the limit of the attitude control capability. Based on thrust-stand data, a thrust vector misalignment was indicated that was slightly higher than permissible for the worst case, i.e., considerable degradation of the torque capacity of the attitude control system combined with venting of helium at its upper limit. The probability of destabilizing the IRAS spacecraft by activating the venting system appeared to be very low. The selection and mounting of the nozzles have satisfied all the requirements for the safe venting of helium.

PRECEDING PAGE BLANK NOT FILMED

SECTION 1

INTRODUCTION

A new Earth-orbiting instrument was assembled that can probe through space seeking celestial phenomena that are invisible to the eye but glow in the infrared. This instrument which has an array consisting of 68 infrared detectors is called the Infrared Astronomical Satellite (IRAS). The heart of IRAS is a 60-centimeter infrared telescope. It is supercooled to 2 K giving it an unprecedented sensitivity to celestial infrared radiation. The telescope and its associated components are cooled by superfluid helium which is carried on the spacecraft in a dewar. After the helium has absorbed thermal energy in the form of sensible heat and latent heat of vaporization, the gaseous helium has to be expelled. Therefore, during the time of its active operation, the Infrared Astronomical Satellite might be exposed to a disturbance torque resulting from venting helium through the Aperture Cover Tank (ACT) Low Thrust Vent (LTV) system. This torque could destabilize the spacecraft if it exceeds the correction capacity of the attitude control system. The torque can be caused by impingement of vented helium on spacecraft surfaces, by asymmetrical positioning of the vent nozzles, by thrust vectors which are not aligned with the ideal nozzle axis and by a difference in the thrust vector magnitude of the two opposing vent nozzles.

The attitude control system employs three identical reaction wheels which are mounted with their axes mutually perpendicular. The reaction wheels exert a maximum attitude control torque of 0.2 Nm on the satellite as well as store an angular momentum of the satellite of at least 14 Nms.

The analysis presented in this report established the upper limits for the misalignment of the two nozzles and the maximum thrust difference between them by evaluating the relative influence coefficients for the attitude control limits in the three axes of the spacecraft.

At the anticipated venting rate the allowable thrust difference between the two vent nozzles could not exceed about 1 percent of the thrust of a single nozzle. Therefore, the selection of two fabricated nozzles could not be based on measured as-machined dimensions and sonic flow rates alone, but confirmation by actual thrust measurements was needed. Differential thrust data for various pairs of five ACT nozzles were generated with the Micropound Extended Range Thrust Stand (MERTS) at the Government Systems Division, Astro-Electronics, of the RCA Corporation in Princeton, New Jersey. The test results were evaluated for their usefulness in establishing the actual maximum thrust mismatch between two selected nozzles and the probable misalignment of the thrust vectors.

SECTION 2

DETERMINATION OF INFLUENCE COEFFICIENTS

2.1 ACT Nozzle

The two ACT nozzles through which helium is to be vented have been designed with the following nominal dimensions:

Throat diameter, inch	0.0612
Exit diameter, inch	0.118
Expansion angle, deg.	15

2.2 Basic Thermodynamic and Fluid Dynamic Relations

The nominal flow rate through each nozzle is given by:

$$\dot{W} = \left\{ (\gamma M/R) [2/(\gamma+1)]^{(\gamma+1)/(\gamma-1)} \right\}^{1/2} A_t p_0 / T_0^{1/2} \quad (1)$$

where	\dot{W}	flow rate, g/sec
	M	molecular weight, g/mole
	R	gas constant, 8.31439×10^7 erg/mole-K
	γ	specific heat ratio of helium, 1.6667
	A_t	throat area, cm^2
	p_0	stagnation pressure, dynes/ cm^2
	T_0	stagnation temperature, K

The nominal thrust produced by each nozzle is given by

$$F = \dot{W} T_0^{1/2} \left\{ [2\gamma R/M(\gamma-1)] [1-(p_e/p_0)^{(\gamma-1)/\gamma}]^{1/2} + (p_e - p_a) A_e \right\} \quad (2)$$

where	F	thrust, dynes
	p_e	exit pressure, dynes/ cm^2
	p_a	ambient pressure, dynes/ cm^2
	A_e	exit nozzle area, cm^2

The nominal exit pressure p_e is found from the relation

$$A_t/A_e = [(\gamma+1)/2]^{1/(\gamma-1)} p_r^{1/\gamma} \left\{ [(\gamma+1)/(\gamma-1)] [1-p_r^{(\gamma-1)/\gamma}]^{1/2} \right\} \quad (3)$$

where	$p_r = p_e/p_0$
-------	-----------------

If the ambient pressure p_a is assumed to be negligibly small, i.e., $p_a = 0$, the nominal thrust F_n of the ACT nozzles is

$$F_n = 9.4135 \times 10^3 \dot{W} T_0^{1/2} \text{ dynes} \quad (4)$$

2.3 Effect of Boundary Layer on Total Thrust

The effect of the boundary layer on the thrust of the ACT nozzles was evaluated with the Boundary Layer Program (Ref.1). The difference between the actual thrust, which takes into account the effect of the boundary layer in the expansion section of the nozzle, and the ideal thrust which is solely based on the above presented ideal thermodynamic and fluid dynamic relations, is shown in Figure 1 as a function of the flow rate \dot{W} . At a flow rate $\dot{W} = 15 \text{ mg/sec}$ the actual thrust might deviate from the ideal thrust by about 10 percent. In Figure 2 the thrust deviation of the actual nozzle thrust from the ideal thrust is shown for two ACT nozzles. The nozzles whose thrust values are being compared vary solely in the length of their expansion section as expressed by the difference in the exit diameters. The difference in length assumed for these calculations is within the indicated machining tolerances for this dimension. The absolute thrust mismatch that could result from the assumed variation in the nozzle exit diameters is shown in Figure 3.

2.4 Influence Coefficients

2.4.1 Coordinates and Coordinate System of IRAS Spacecraft

The two ACT nozzles have been placed on the spacecraft as indicated in Figure 4. The axes of the two nozzles lie parallel to the y-axis of the spacecraft, i.e., the inclination θ to the x-z plane is zero degree and the inclination ϕ to the x-axis in the x-y plane equals $+90^\circ$ and -90° respectively. The coordinates of the centers of the nozzle exit planes are given in Table 1 with the location of the center of mass of the spacecraft.

	x, cm	y, cm	z, cm
Nozzle #1	297	101	0.0
Nozzle #2	297	-101	0.0
Center of Mass	124.1	-1	1.2

Table 1 Coordinates of the ACT Nozzles and the Center of Mass of the IRAS Spacecraft

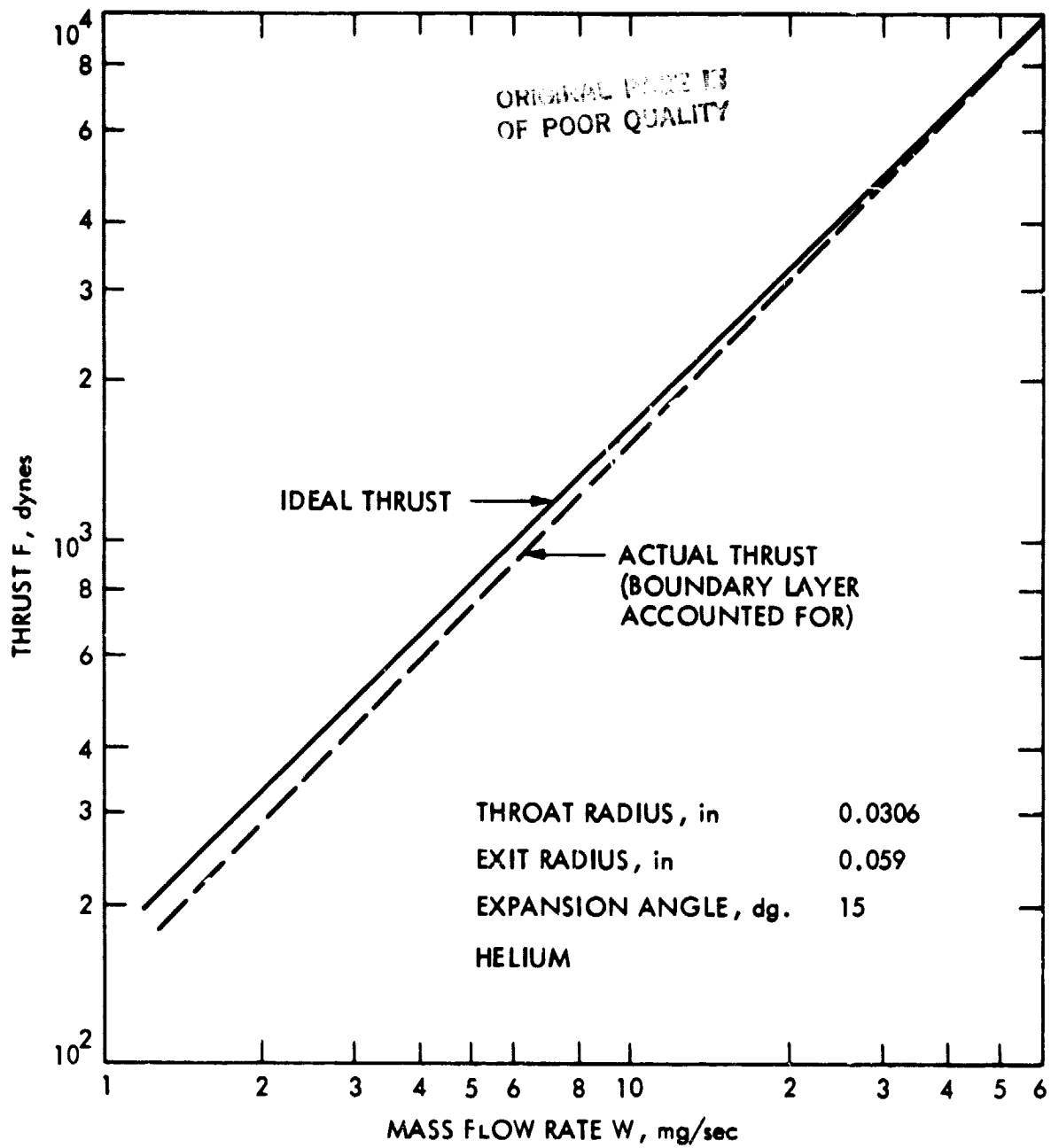


Figure 1 ACT Nozzle Thrust Characteristic

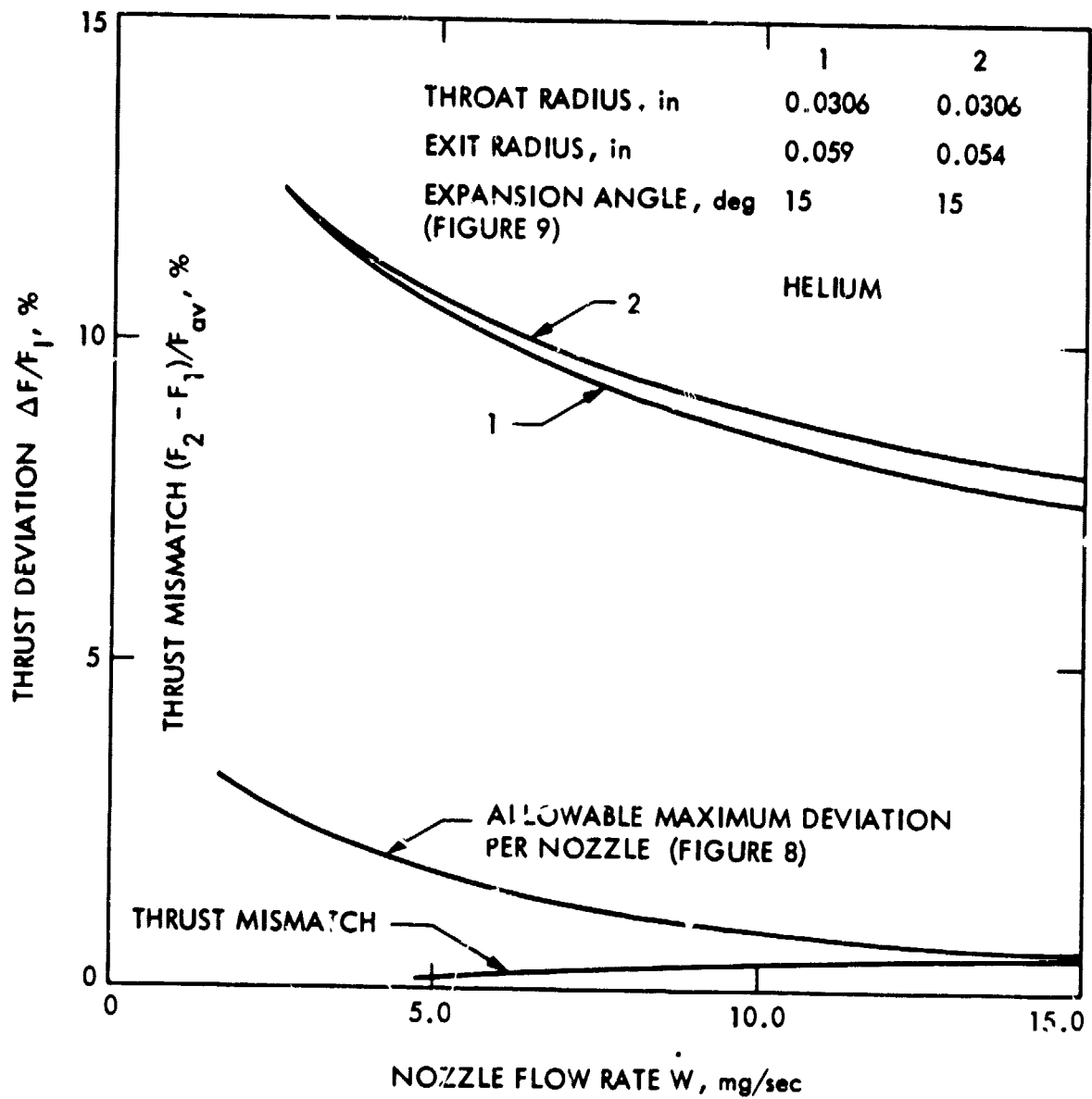


Figure 2 Deviation from Ideal Thrust Due to Boundary Layer

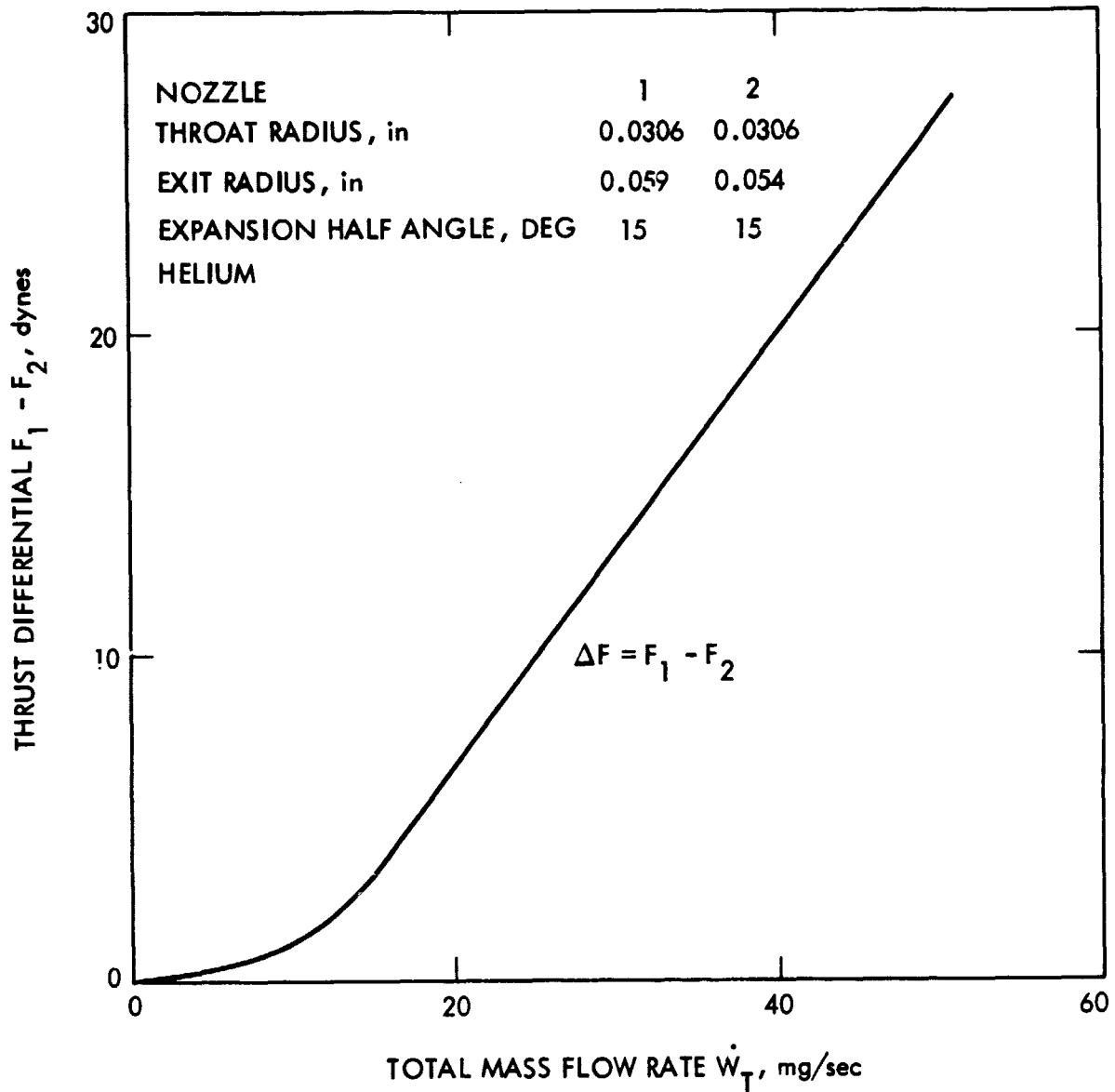


Figure 3 Analytically Predicted Thrust Differential

ORIGINAL PAGE IS
OF POOR QUALITY

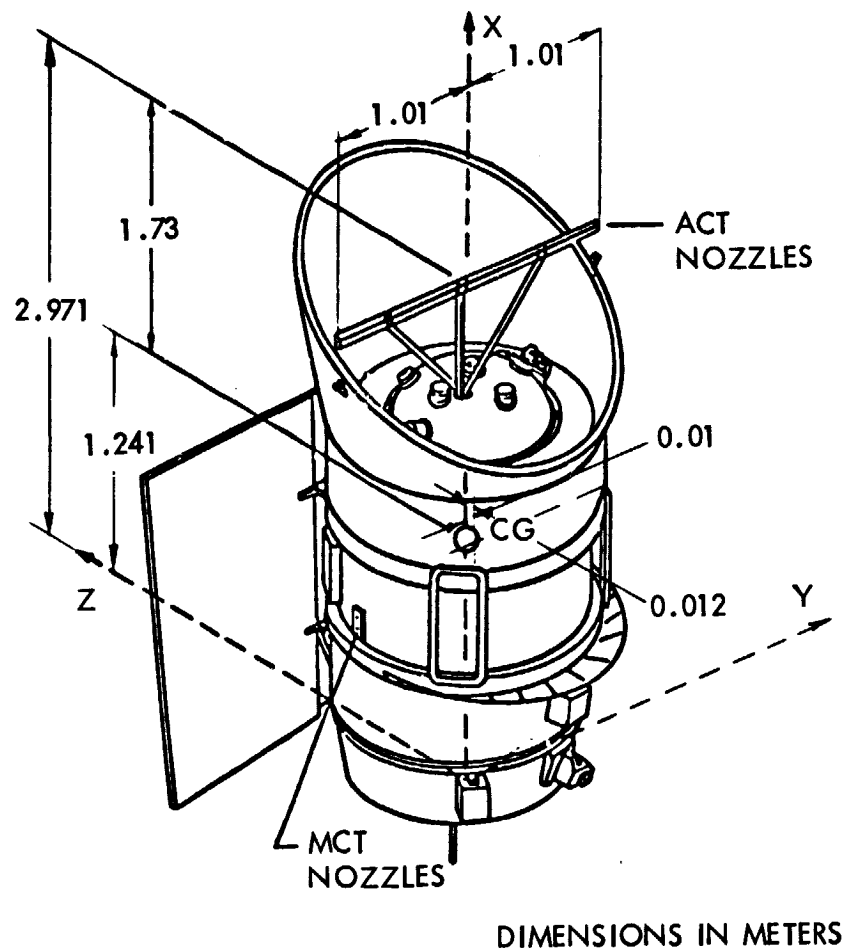


Figure 4 IRAS Spacecraft Coordinate System

During venting of helium through the two nozzles the spacecraft's attitude will remain undisturbed only, if the torques around each of the three axes which are produced by the two nozzles are equal and opposite to each other. In order to achieve this ideal condition the nozzles are to be located such that their axes lie parallel to the y-axis at an equal distance from the x-z plane. Furthermore the two nozzles were to have the same physical configurations so that the flow rate as well as the expansion ratio would be equal, thus producing the same thrust at a given total flow rate \dot{W}_T of helium.

The ideal conditions of perfect alignment and equal thrust of two nozzles can be realized only within the limits achievable by machining accuracy and specified tolerances. Therefore, the torque due to deviations from ideal alignment and nominal size of the thrust vectors has to be evaluated by determining the influence coefficients for each of the three parameters, the inclination θ from the x-y plane, the inclination ϕ from the x-axis in the x-y plane, and the deviation from the nominal thrust F_n . The transformation equations and their derivation for transforming the spherical coordinate angles θ and ϕ to the coordinate angles α and β , where α is the cone angle and β is the clock angle for the nozzle, are presented in Appendix A.

2.4.2 Torques Around the Three Major Spacecraft Axes

The torques around the three major coordinate axes, T_x , T_y , and T_z , which are due to the thrust F_n of nozzle n are

$$T_{nx} = F_{ny}(z_n - z_c) + F_{nz}(y_n - y_c) \quad (5a)$$

$$T_{ny} = F_{nz}(x_n - x_c) + F_{nx}(z_n - z_c) \quad (5b)$$

$$T_{nz} = F_{nx}(y_n - y_c) + F_{ny}(x_n - x_c) \quad (5c)$$

where the x, y, z components of the thrust vector F_n are given by

$$F_{nx} = F_n \cos \theta_n \cos \phi_n \quad (6a)$$

$$F_{ny} = F_n \cos \theta_n \sin \phi_n \quad (6b)$$

$$F_{nz} = F_n \sin \theta_n \quad (6c)$$

By inserting relations 6a, 6b and 6c into relations 5a, 5b and 5c the final torque relations for the three major axes are given by

$$T_{nx} = F_n [(y_n - y_c) \sin \theta_n + (z_n - z_c) \cos \theta_n \sin \phi_n] \quad (7a)$$

$$T_{ny} = F_n [(z_n - z_c) \cos \theta_n \cos \phi_n + (x_n - x_c) \sin \theta_n] \quad (7b)$$

$$T_{nz} = F_n [(x_n - x_c) \cos \theta_n \sin \phi_n + (y_n - y_c) \cos \theta_n \cos \phi_n] \quad (7c)$$

ORIGINAL PAGE IS
OF POOR QUALITY

By partial differentiation of relation 7a with respect to the three variables, F_n , θ_n and ϕ_n the following relation is obtained

$$\begin{aligned} dT_{nx} = & [(y_n - y_c)\sin\theta_n + (z_n - z_c)\cos\theta_n\sin\phi_n]dF_n \\ & + F_n[(y_n - y_c)\cos\theta_n - (z_n - z_c)\sin\theta_n\sin\phi_n]d\theta_n \\ & + F_n(z_n - z_c)\cos\theta_n\cos\phi_n d\phi_n \end{aligned} \quad (8)$$

When setting the differentials of relation 8 equal to the differences and considering that

$$\theta_n = 0^\circ \quad (9a)$$

and

$$\phi_n = \pm 90^\circ \quad (9b)$$

$$\Delta T_{nx} = F_n(y_n - y_c)\Delta\theta_n + (z_n - z_c)\Delta F_n \quad (10a)$$

Similarly, the differential torques around the y-axis and the z-axis can be derived.

$$\Delta T_{ny} = -F_n(z_n - z_c)\Delta\phi_n + F_n(x_n - x_c)\Delta\theta_n \quad (10b)$$

$$\Delta T_{nz} = (x_n - x_c)\Delta F_n - F_n(y_n - y_c)\Delta\theta_n \quad (10c)$$

From relations 10a, 10b and 10c the absolute influence coefficients C_{imF} , $C_{im\theta}$ and $C_{im\phi}$ for the three major variables of each nozzle are found to be as shown in Table 2.

Torque Deviant	T_{nx}	T_{ny}	T_{nz}
ΔF_n	$(z_n - z_c)$		$(x_n - x_c)$
$\Delta\theta_n$	$F_n(y_n - y_c)$	$F_n(y_n - y_c)$	
$\Delta\phi$		$F_n(z_n - z_c)$	$F_n(y_n - y_c)$

Table 2 Influence Coefficients of the Three Major Nozzle Parameters

The torque around a single axis can be generated by a positive deviation, i.e., a thrust increase of ΔF_n as well as a negative deviation, i.e., a thrust decrease of ΔF_n . Whether the thrust deviation is positive or negative the resulting torque due

to the deviation of a single nozzle cannot be permitted to exceed one half the attitude control capacity T_c of the spacecraft for a given axis. When setting the torque induced by a single nozzle deviation equal to one half of the torque correction capacity T_c , i.e.,

$$\Delta T_{nm} = T_c/2 \quad (11)$$

and substituting this into relations 10a, 10b, and 10c, the absolute values for the maximum allowable deviations of the three parameters are established. These absolute values for the three parameters, the thrust F_n , the inclination θ_n , and the inclination ϕ_n , are tabulated in Table 3.

Torque Deviant	T_{nx}	T_{ny}	T_{nz}
ΔF_n , dynes	$T_{cx}/(z_n - z_c)$		$T_{cz}/(x_n - x_c)$
$\Delta F_n/F_n$	$T_{cx}/\{F_n(z_n - z_c)\}$		$T_{cz}/\{F_n(x_n - x_c)\}$
$\Delta \theta_n$, deg.	$T_{cx}/\{F_n(y_n - y_c)\}$	$T_{cy}/\{F_n(x_n - x_c)\}$	
$\Delta \phi_n$, deg.		$T_{cy}/\{F_n(z_n - z_c)\}$	$T_{cz}/\{F_n(y_n - y_c)\}$

Table 3 Allowable Deviations for the Three Major Nozzle Parameters

The most general expression for relating the maximum deviations of the three major parameters, ΔF_n , $\Delta \theta_n$ and $\Delta \phi_n$, for the three axes of the spacecraft with the control capacity of the spacecraft is

$$T_{cm} = C_{imF}\Delta F_n + C_{im\theta}\Delta \theta_n + C_{im\phi}\Delta \phi_n \quad (12)$$

where

$$m = x, y, z$$

The maximum allowable deviations and their combinations of the three major variables F_n , θ_n , and ϕ_n for the three torque axes of the spacecraft are presented graphically for an attitude control capability $T_c = 5 \times 10^3$ dynes-cm in Figures 5 through 8.

ORIGINAL PAGE IS
OF POOR QUALITY

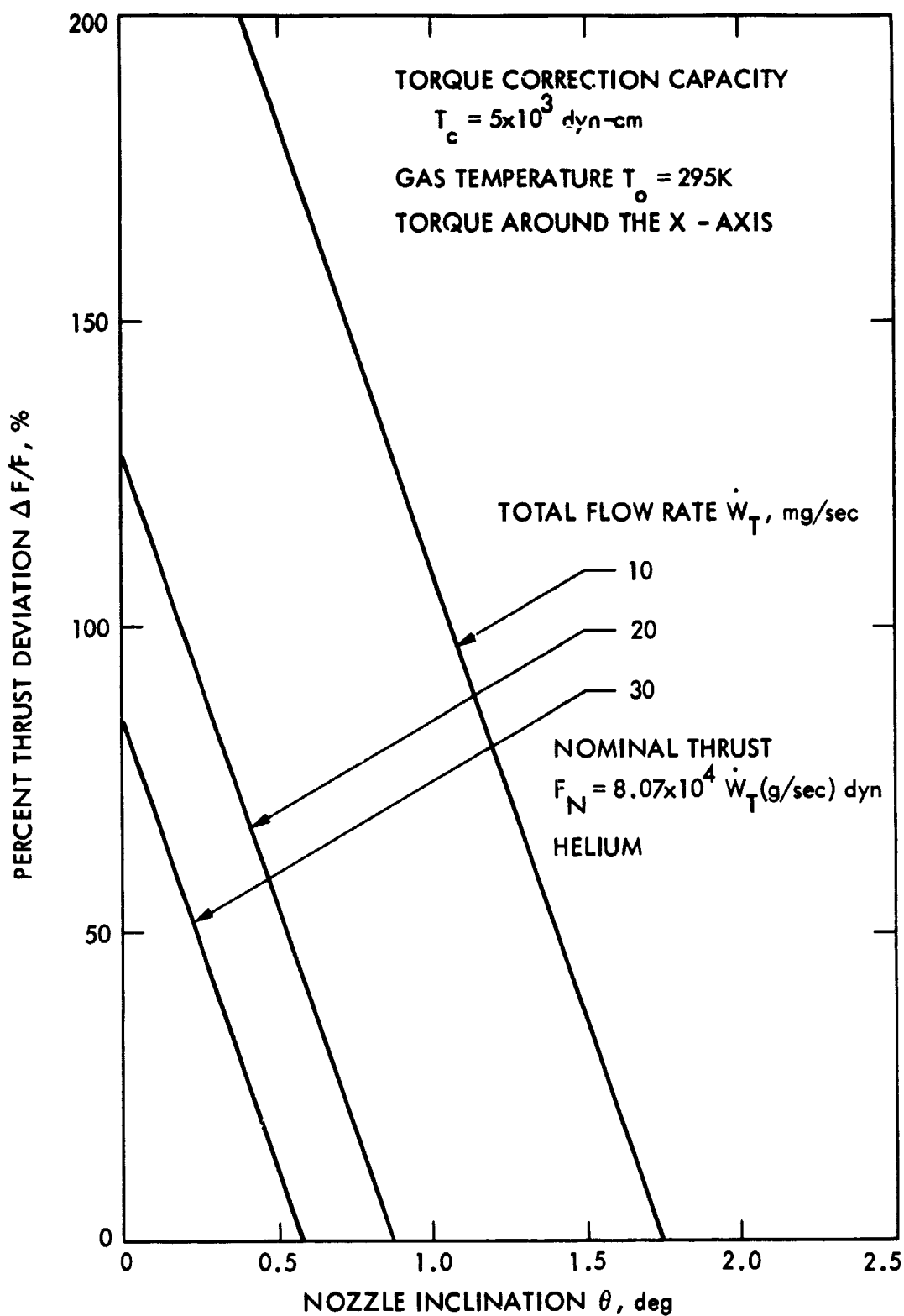


Figure 5 Upper Bound for Torque Around the X - Axis

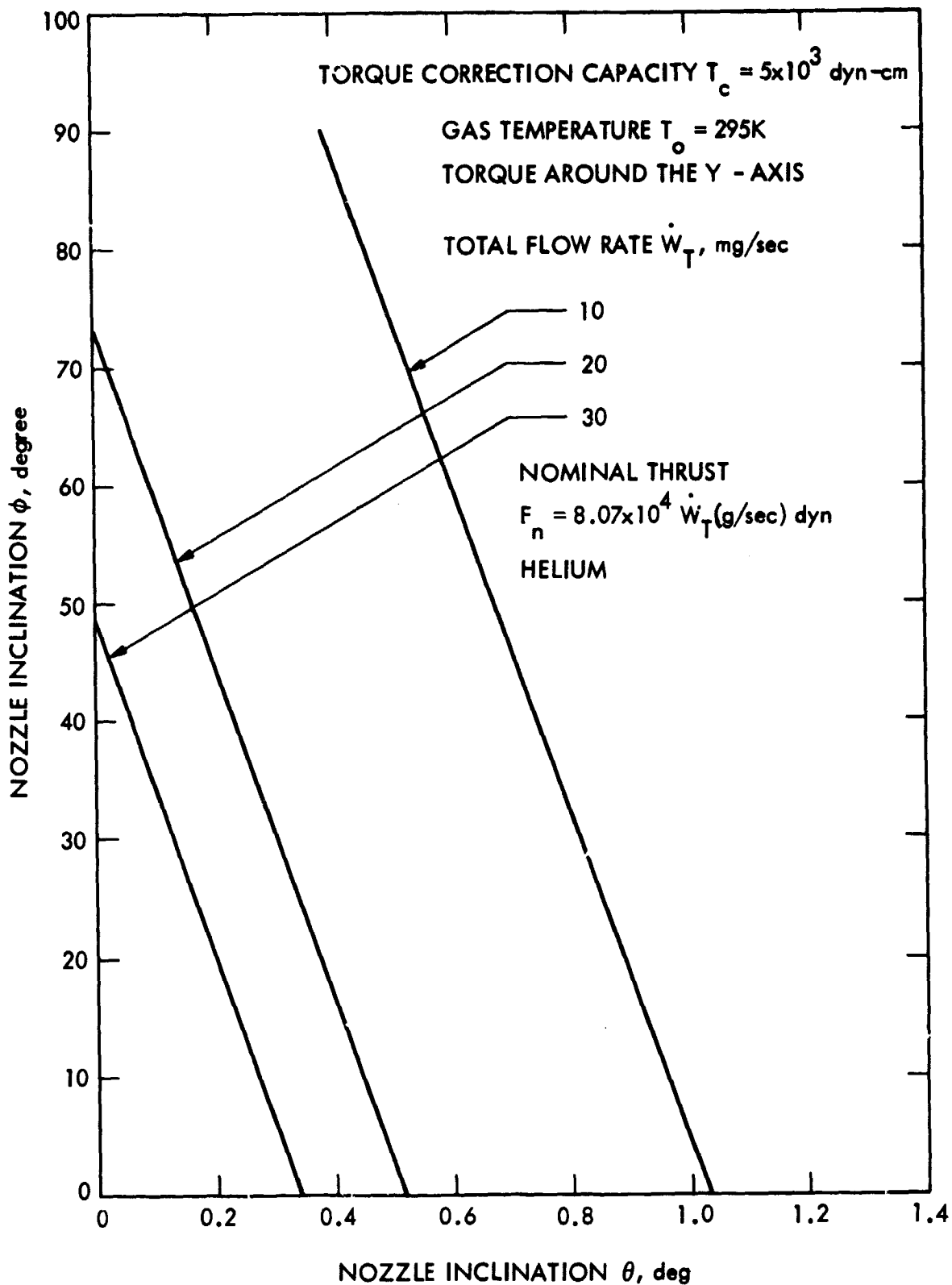


Figure 6 Upper Bound for Torque Around the Y - Axis

ORIGINAL PAGE IS
OF POOR QUALITY

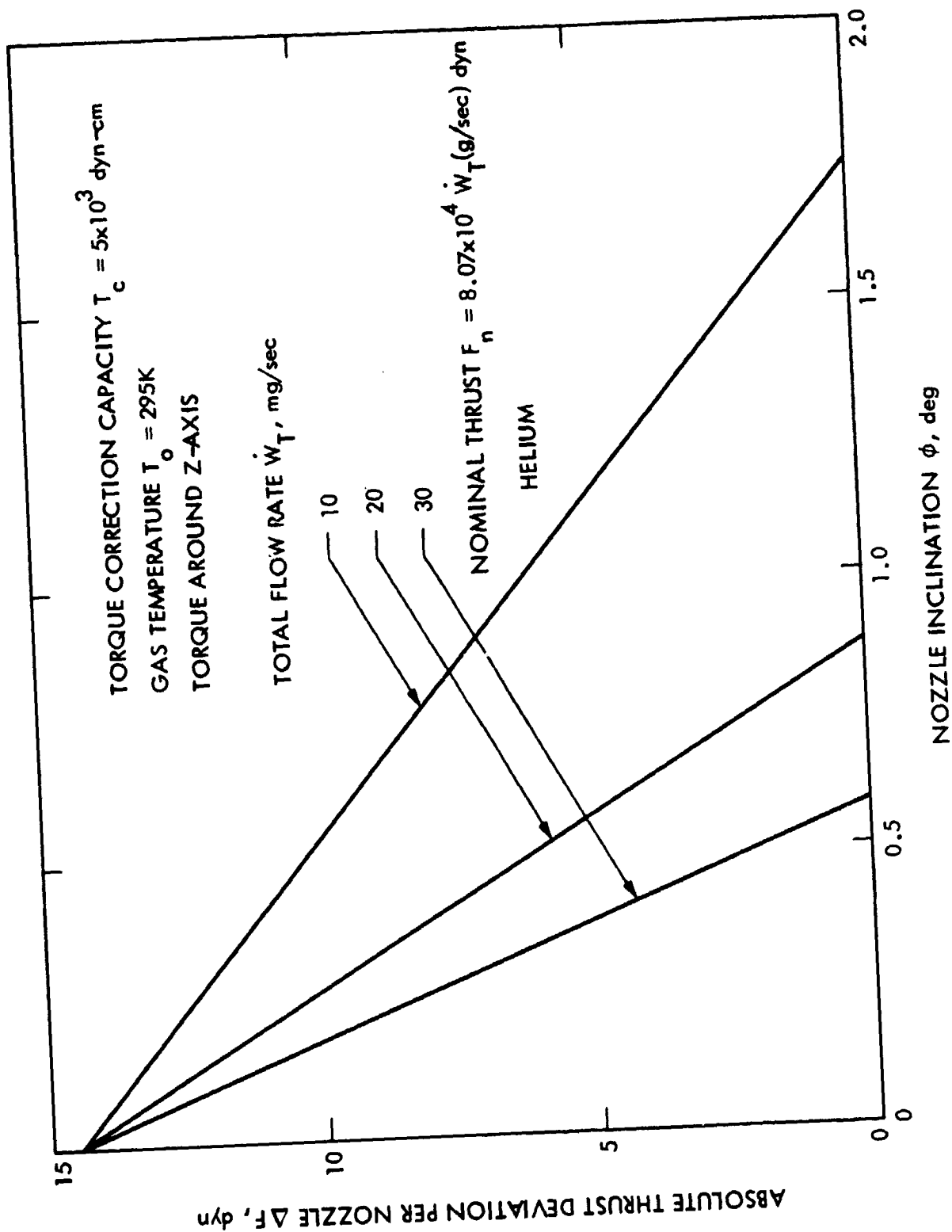


Figure 7 Upper Bounds for Torque Around the Z-Axis (ΔF and ϕ)

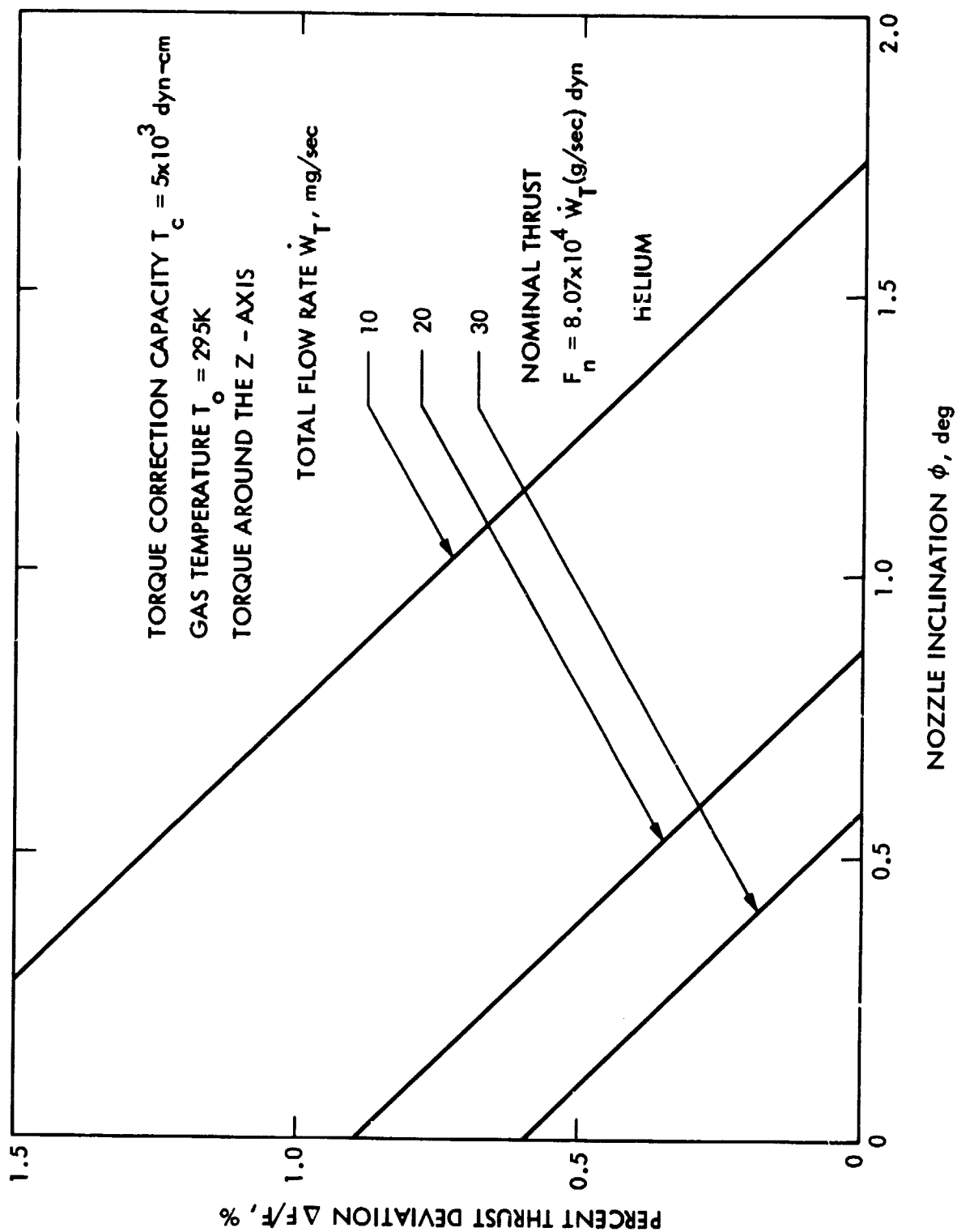


Figure 8 Upper Bound for Torque Around the Z-Axis ($\Delta F/F$ and ϕ)

SECTION 3

EXPERIMENTAL EVALUATION OF ACT NOZZLES

3.1 General Approach

In section 2 of this report the maximum permissible deviations of the three major nozzle parameters, the absolute thrust F_n and the two angular deviations from the nominal thrust vector direction, θ_n and ϕ_n , as imposed by the limited capability of the attitude control of the spacecraft were evaluated. It was shown that at a total vent flow rate $\dot{W}_T = 30$ mg/sec the absolute thrust deviation per nozzle, ΔF_n , could not exceed 14.4 dynes or 0.6 percent of the nominal thrust. The angular deviation θ from the y-axis has to be limited to $\Delta\theta = 0.58$ degree and the angular inclination to the x-y plane cannot be greater than $\Delta\theta = 0.34$ degree. These are individually imposed limits and are the upper limits only if and when neither of the other two parameters deviates concurrently.

Five nozzles were built by the vendor which were to be evaluated for their usefulness on the IRAS spacecraft. Two methods were employed for finding the best match between a pair of nozzles, i.e., two nozzles which would produce the smallest difference between their thrust and appear to have thrust vectors which deviate least from the physical nozzle axis. In the first method the mass flow rate \dot{W}_n of each nozzle was established as a function of the supply pressure p_o . The second method employed a thrust stand which was believed to be capable of measuring accurately an absolute thrust of less than 5 μ lb. This thrust level had been determined to be the maximum allowable thrust difference between the matched nozzle pair that was to be mounted on the spacecraft.

3.2 Nozzle Evaluation by Sonic Flow Measurement

Five nozzles were manufactured. They were machined to the dimensions and tolerances as shown in Figure 9 with a nominal throat diameter of $D_n = 0.0612$ inch. The nozzles were identified by their serial numbers from S/N001 through S/N005.

Each nozzle was evaluated for its sonic flow as function of the upstream pressure at room temperature. The measured relations between stagnation pressure and mass flow rate are shown in Table 4 and Figure 10.

According to relation 2 the ideal thrust is a function of the mass flow rate W , the stagnation pressure p_o , the exit pressure p_e and the stagnation temperature T_o . Since both nozzles of the helium vent system are fed from the same manifold, the difference in their thrust is primarily a function of the flow rate through each nozzle.

ORIGINAL PAGE 19
OF POOR QUALITY

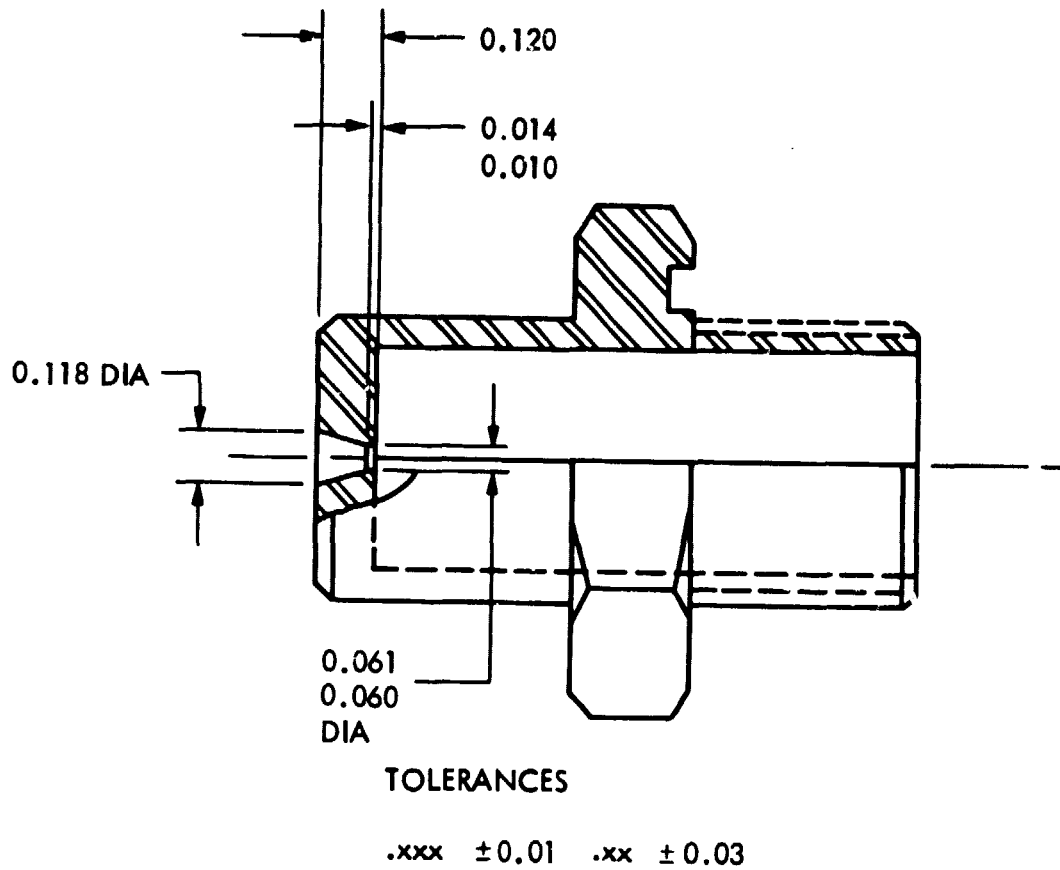


Figure 9 ACT Nozzle Design

Nozzle	Data		Least Square Fit	
	Pressure torr	Flow Rate mg/sec	Slope mg/sec/torr	Intersection mg/sec
S/N001	0.0	0.0	0.21268	-0.322
	12.04	2.2912		
	26.42	5.2887		
	54.00	11.069		
	93.20	19.550		
S/N002	0.0	0.0	0.20825	-0.248
	12.03	2.2705		
	26.50	5.2396		
	54.06	11.036		
	93.27	19.168		
S/N003	0.0	0.0	0.20342	-0.227
	12.15	2.2377		
	26.49	5.1643		
	54.00	10.766		
	93.12	19.168		
S/N004	0.0	0.0	0.20734	-0.259
	12.12	2.2547		
	26.24	5.1554		
	53.70	10.920		
	93.04	19.014		
S/N005	0.0	0.0	0.20933	-0.314
	12.08	2.2382		
	25.88	5.0704		
	53.88	10.950		
	93.17	19.202		

Table 4 Sonic Flow Measurements of Nozzles 64874-5

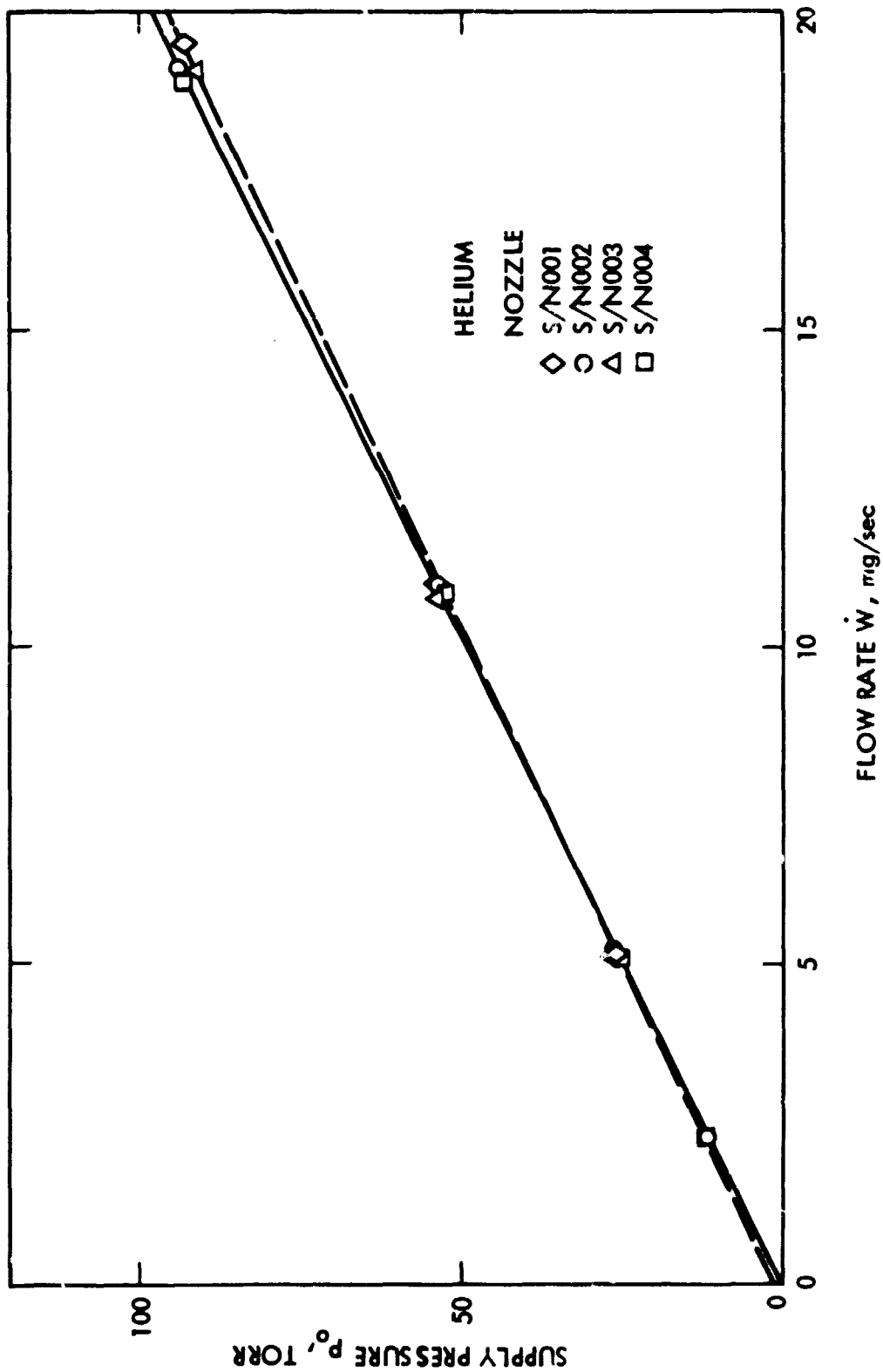


Figure 10 Nozzle Calibration of ACT Vent Nozzles #64874-5

ORIGINAL PAGE IS
OF POOR QUALITY

$$F_n = C_f \dot{W}_n \quad (13)$$

where C_f thrust coefficient common to both nozzles, dynes/(g/sec)

The sum of the two flow rates has to equal the total vent flow \dot{W}_T

$$\dot{W}_T = \dot{W}_1 + \dot{W}_2 \quad (14)$$

where the individual flow rates \dot{W}_n are a function of the upstream pressure p_o and the flow coefficient m_n as defined in Table 4.

$$\dot{W}_n = m_n p_o \quad (15)$$

By inserting relation 15 into relation 14 the total flow rate is found to be

$$\dot{W}_T = p_o (m_1 + m_2) \quad (16)$$

The thrust mismatch between two nozzles is

$$\Delta F = C_f (\dot{W}_1 - \dot{W}_2) \quad (17)$$

By employing again relation 15 in relation 17

$$\Delta F = C_f p_o (m_1 - m_2) \quad (18)$$

The total pressure p_o is from relation 16

$$p_o = \dot{W}_T / (m_1 + m_2) \quad (19)$$

By replacing relation 19 in relation 18

$$\Delta F = C_f \dot{W}_T (m_1 - m_2) / (m_1 + m_2) \quad (20)$$

For a nominal thrust coefficient C_f

$$C_f = 347.3 \text{ } \mu\text{lb}/(\text{mg}/\text{sec})$$

$$C_f = 154.48 \text{ dynes}/(\text{mg}/\text{sec})$$

and a total vent flow $\dot{W}_T = 30 \text{ mg}/\text{sec}$ the following thrust mismatches between nozzle S/N001 and the remaining four nozzles can be calculated.

$$\Delta F_{1-2} = 109.57 \text{ } \mu\text{lb}$$

$$\Delta F_{1-3} = 231.92 \text{ } \mu\text{lb}$$

$$\Delta F_{1-4} = 132.48 \text{ } \mu\text{lb}$$

$$\Delta F_{1-5} = 82.72 \text{ } \mu\text{lb}$$

A graphical representation of the theoretical thrust mismatches is given in Figure 11. From these theoretical values the smallest thrust mismatch should be achieved with the nozzle pair S/N002 and S/N004, i.e.,

$$\begin{aligned}\Delta F_{2-4} &= 22.81 \text{ } \mu\text{lb} \\ &= 10.15 \text{ dynes}\end{aligned}$$

The magnitude of this thrust mismatch is 0.437 percent of the nominal thrust per nozzle $F_n = 2,317$ dynes in an environment with an ambient pressure equal to the nominal exit pressure of the nozzle. The exit pressure of the nominal nozzle is

$$p_e = 0.02545 p_o$$

The total thrust is the sum of the momentum exchange and the pressure differential across the exit plane of the nozzle. For the nominal nozzle the thrust is thus

$$F = F_m + F_{\Delta p} \quad (21)$$

$$\text{where} \quad F_m = 8.94 \times 10^3 \dot{W}_{nT_o}^{1/2} \quad (22)$$

$$F_{\Delta p} = 4.695 \times 10^2 \dot{W}_{nT_o}^{1/2} \quad (23)$$

From relations 22 and 23 it is seen that for the nozzles under consideration the thrust which can be attributed to the pressure differential across the exit plane of the nozzle contributes only 5 percent to the total thrust. If accounted for this component of the thrust would have only a minor influence on the analysis which assumes an ambient pressure equal to the exit pressure of the nominal nozzle.

The thrust mismatch $\Delta F = 10.15$ dynes would mean a deviation of $\Delta F_n = 5.08$ dynes per nozzle at a total vent flow rate $\dot{W}_T = 30$ mg/sec. The tightest tolerance on the thrust is demanded for limiting the torque around the z-axis. According to Figure 7 the nozzle pair is within the established tolerance for both parameters, F_n and θ_n , if each nozzle's thrust vector is aligned within $\theta = 0.375$ degree of the y-axis. The largest permissible misalignment of each thrust vector $\theta = 0.58$ degree is only acceptable with a perfect thrust match between the two nozzles, i.e., $\Delta F = 0.0$.

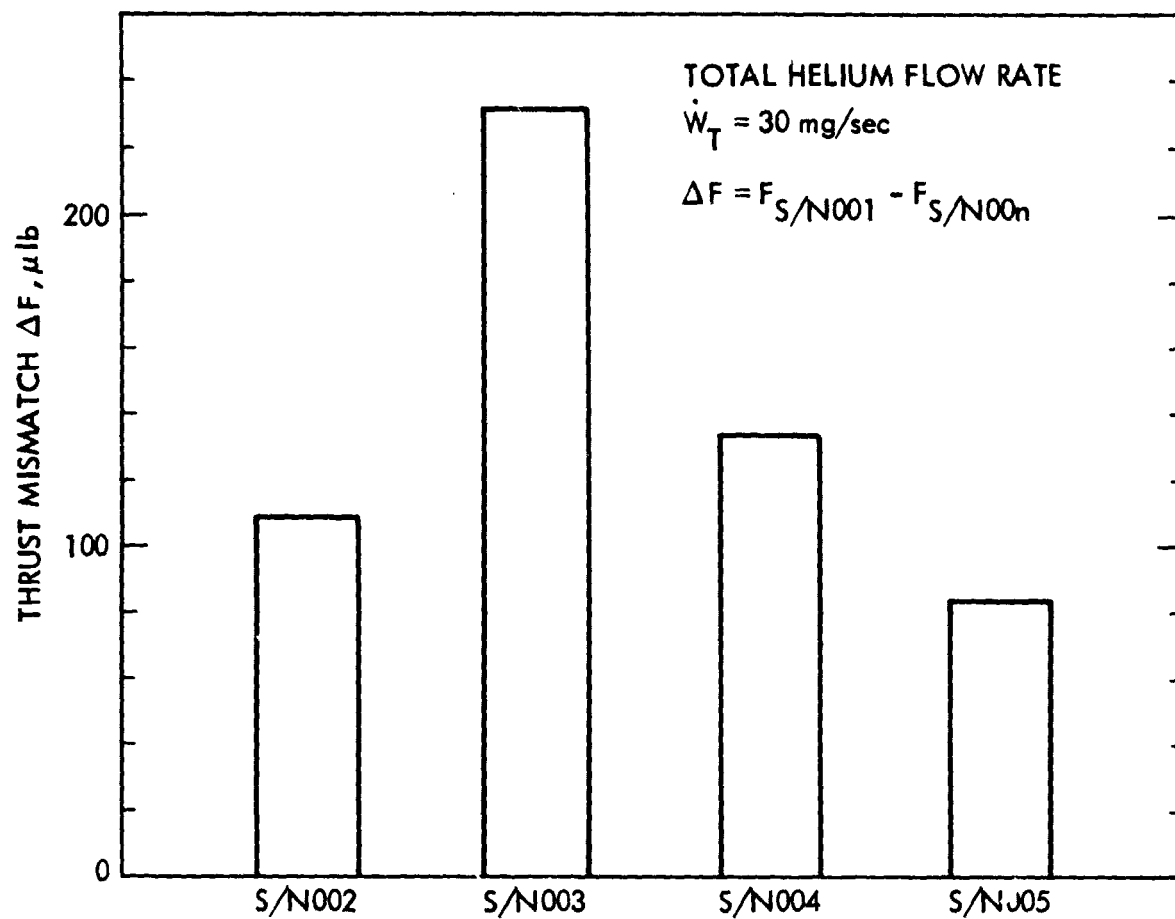


Figure 11 Calculated Thrust Mismatch Between Nozzle S/N001 and Nozzles S/N002 through S/N005

3.3 Testing of ACT Nozzles on MERTS Thrust Measuring Stand

The evaluation of the nozzles based on the sonic flow rate was not considered adequate for determining the possible thrust mismatch between two nozzles. It was therefore decided to test the nozzles on the MERTS thrust measuring stand and generate absolute thrust difference values for a selected pair of nozzles.

The MERTS thrust stand is a device which was designed and built to measure thrust vectors of the order of 1 μ lb. It indicates the linear displacement of a beam which rotates due to a thrust force at its end. The thrust measuring device is therefore not measuring the absolute thrust of a jet, but the torque resulting from a thrust vector whose origin is located at the end of the beam. Normally the assumption is made that the thrust vector is perpendicular to the beam and thus parallel to the magnetic force or the pull of a weight which are used for calibrating the thrust stand during testing.

Instead of mounting a single fully self-contained thrust unit on the thrust stand, a manifold with two opposing nozzles was attached to the platform and a Teflon tube was added to the thrust device to carry helium from the outside of the vacuum tank to the manifold. By adding Teflon tubing to the setup a basic change in the thrust measuring device was introduced. A resistance to the restoring torque of the thrust balance was added whose absolute value and linearity were not known. The MERTS thrust stand had been designed and operated specifically without leads of any kind crossing the torque joint. The test data which were obtained during testing of the ACT nozzles on this thrust stand are therefore not consistent. Most of the thrust values deduced from the data appear to lie within the noise level of the thrust indication of the modified thrust stand.

The accuracy of the thrust measuring device in its modified configuration is demonstrated by the correlation between the calibration force and the displacement transducer output as shown in Figure 12. With a calibration force of 10 μ lb the transducer output indicated from 4.5 to 7.3 divisions on the strip chart at a mean of 6 divisions. The accuracy of the indicated thrust can therefore not be better than 46.67 percent in the thrust regime of interest. The least consistency in the thrust indication is observed when it was negative, i.e., opposite to the thrust indication of the calibration force. This is shown by the correlation of the thrust mismatch between nozzles S/N001 and S/N002. In the first test the two nozzles were arranged to produce a positive thrust indication, nozzle S/N001 having the higher thrust level. In the second immediately following test the thrust indication was negative at all flow rates because the two nozzles had been interchanged in the manifold. The results of these two tests are shown in Figure 13.

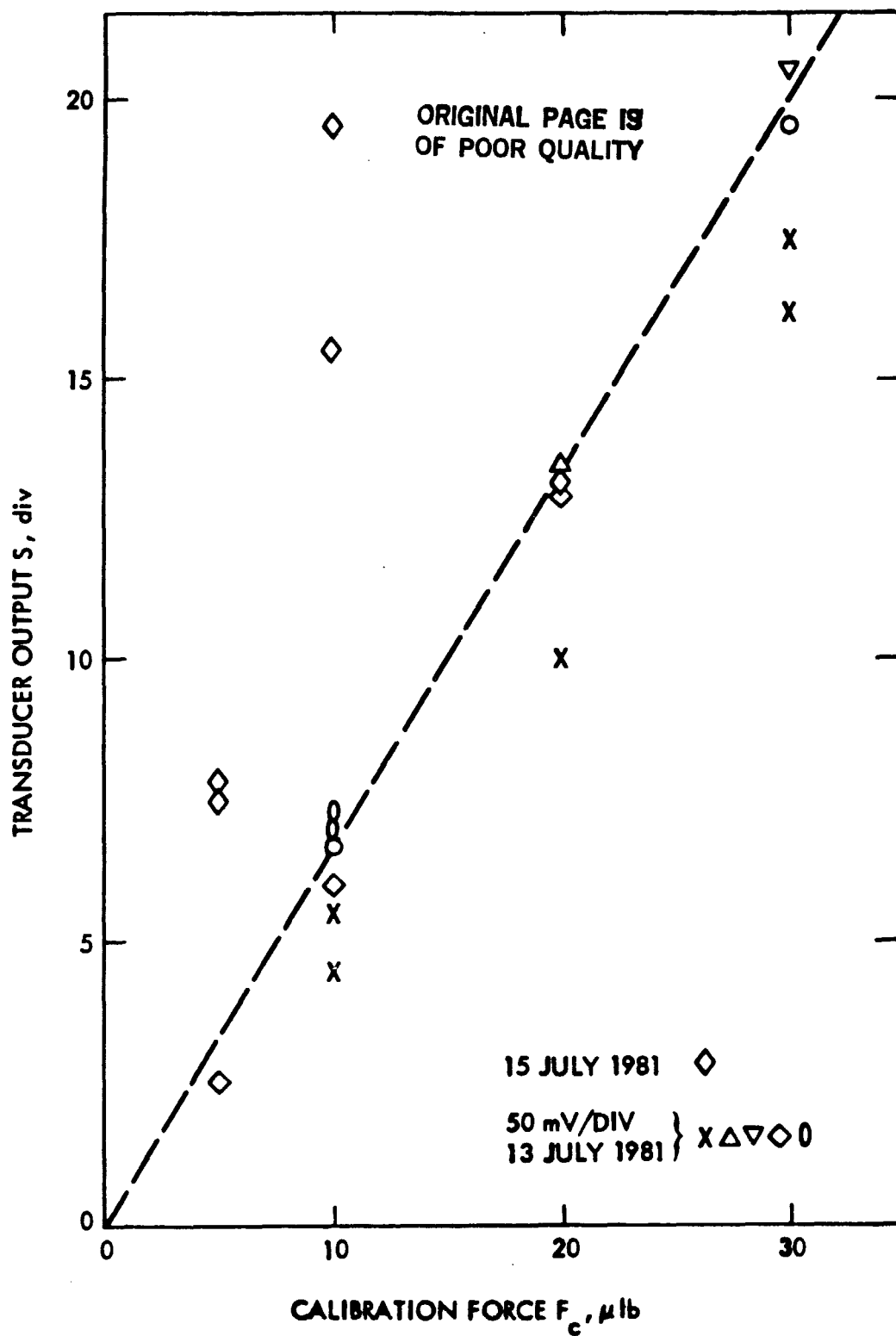


Figure 12 Repeatability of Calibration of Micropound Thrust Stand (MERTS)

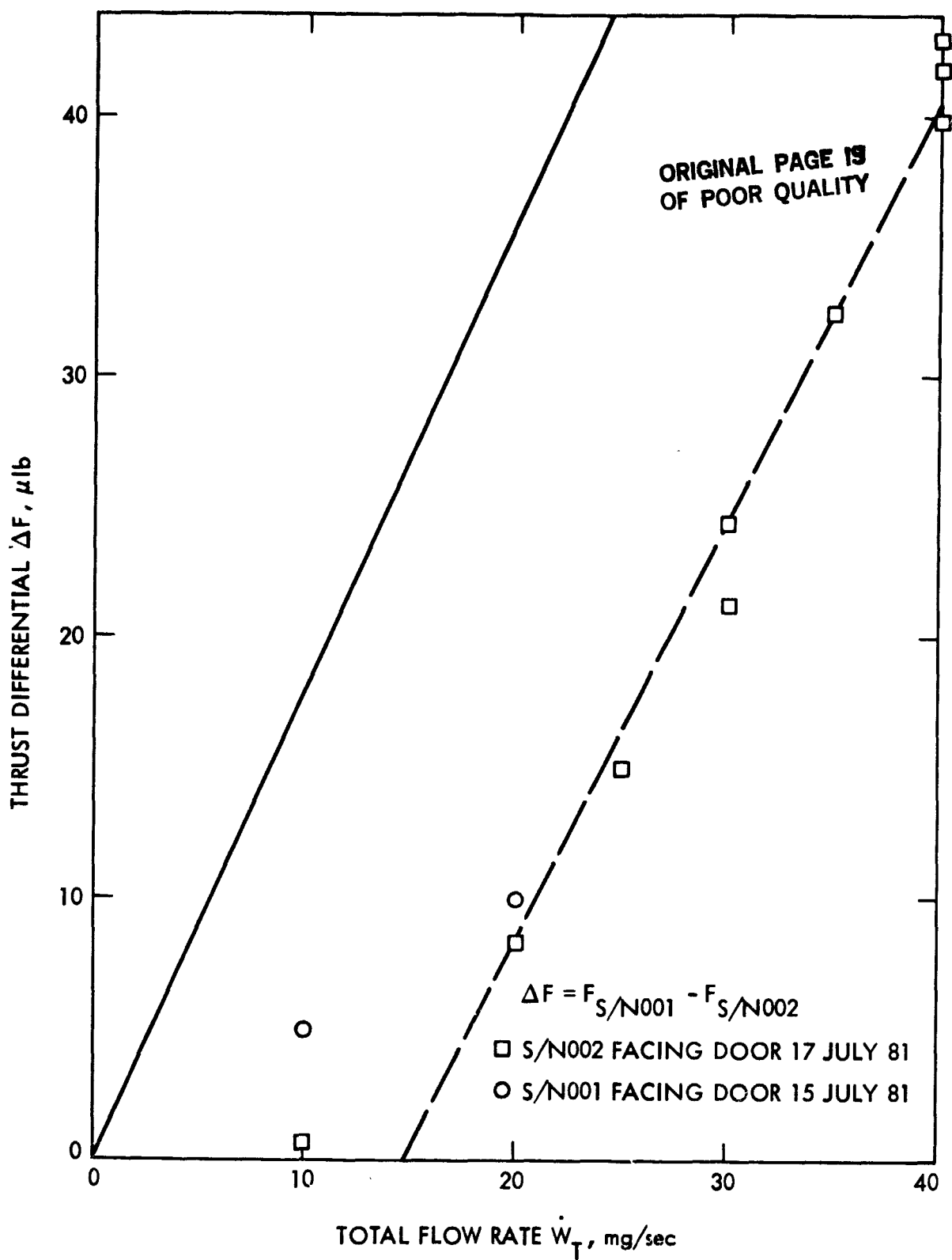


Figure 13 Indicated Thrust Mismatch Between Nozzles
S/N001 and S/N002

In a third test series these two nozzles were tested again for evaluating the thermal effects on the nozzle thrust balance at a total flow rate $\dot{W}_T = 20$ mg/sec. The results of this test are shown in Figure 14. The data appear to be very consistent and reveal that when nozzle S/N001 is exposed to heat, the thrust mismatch between the two nozzles will change according to the relation

$$\Delta(\Delta F_T) = -0.8127 \Delta T$$

where ΔT change of temperature of nozzle S/N001, K

When nozzle S/N002 was heated the thrust difference increased by the relation

$$\Delta(\Delta F_T) = 0.8916 \Delta T$$

In this test series the indicated thrust mismatch between the two nozzles was only about $\Delta F_{1-2} = 6$ μ lb when both nozzles were at room temperature. This compares with the thrust mismatch of $\Delta F_T = 8.5$ μ lb which was measured in previous tests. These test results seem to confirm that the absolute thrust could not be measured with an accuracy of better than 42 percent at these low differential thrust levels.

In a test series which was designed to determine the thrust mismatches of all nozzles with respect to nozzle S/N001 when venting 30 mg/sec of helium, the thrust differences as shown in Figure 15 were measured. From the differences ΔF_{1-3} and ΔF_{1-4} a thrust mismatch between nozzles S/N003 and S/N004 of $\Delta F_{4-3} = 20.5$ dynes is indicated. This agrees quite well with the test data shown in Figure 16 when the two nozzles were directly compared on the thrust stand.

In Figure 17 the test results obtained during the direct comparison test between nozzles S/N002 and S/N004 are presented. When the two nozzles are mounted in the thrust stand such that the resulting indicated thrust is negative, the test data are very inconsistent. However, when the indicated thrust is positive a good correlation between thrust mismatch and total flow rate was generated. At a total flow rate $\dot{W}_T = 30$ mg/sec an apparent thrust mismatch between this nozzle pair $\Delta F_{2-4} = 7.3$ μ lb (3.25 dynes) was indicated. From the indirect evaluation of the thrust mismatch between these two nozzles, as was shown in Figure 15, a thrust difference of only $\Delta F_{2-4} = 1$ μ lb would have been predicted.

ORIGINAL PAGE IS
OF POOR QUALITY

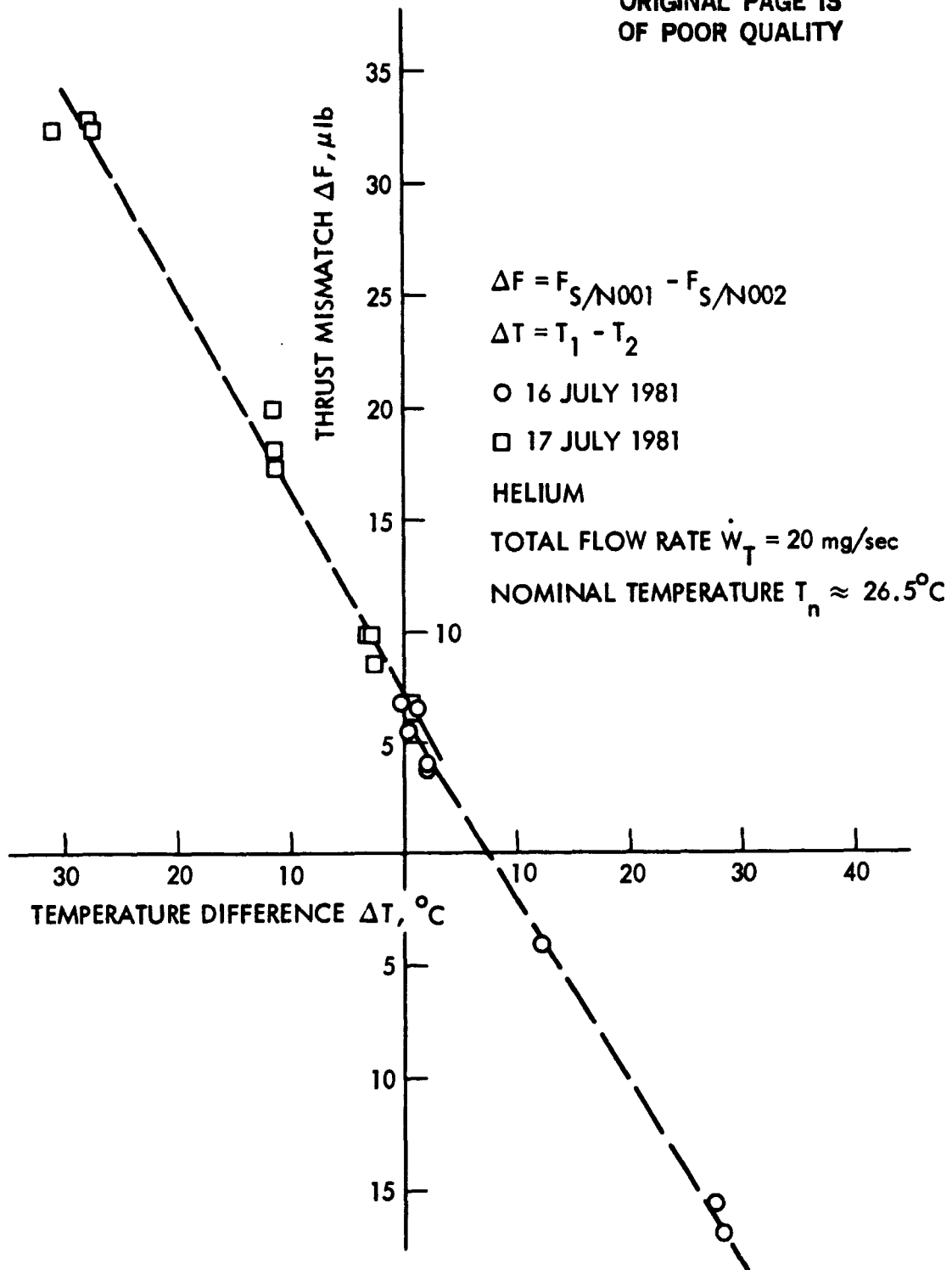


Figure 14 Thrust Mismatch Between Two Nozzles Due to Temperature Difference

ORIGINAL PAGE IS
OF POOR QUALITY

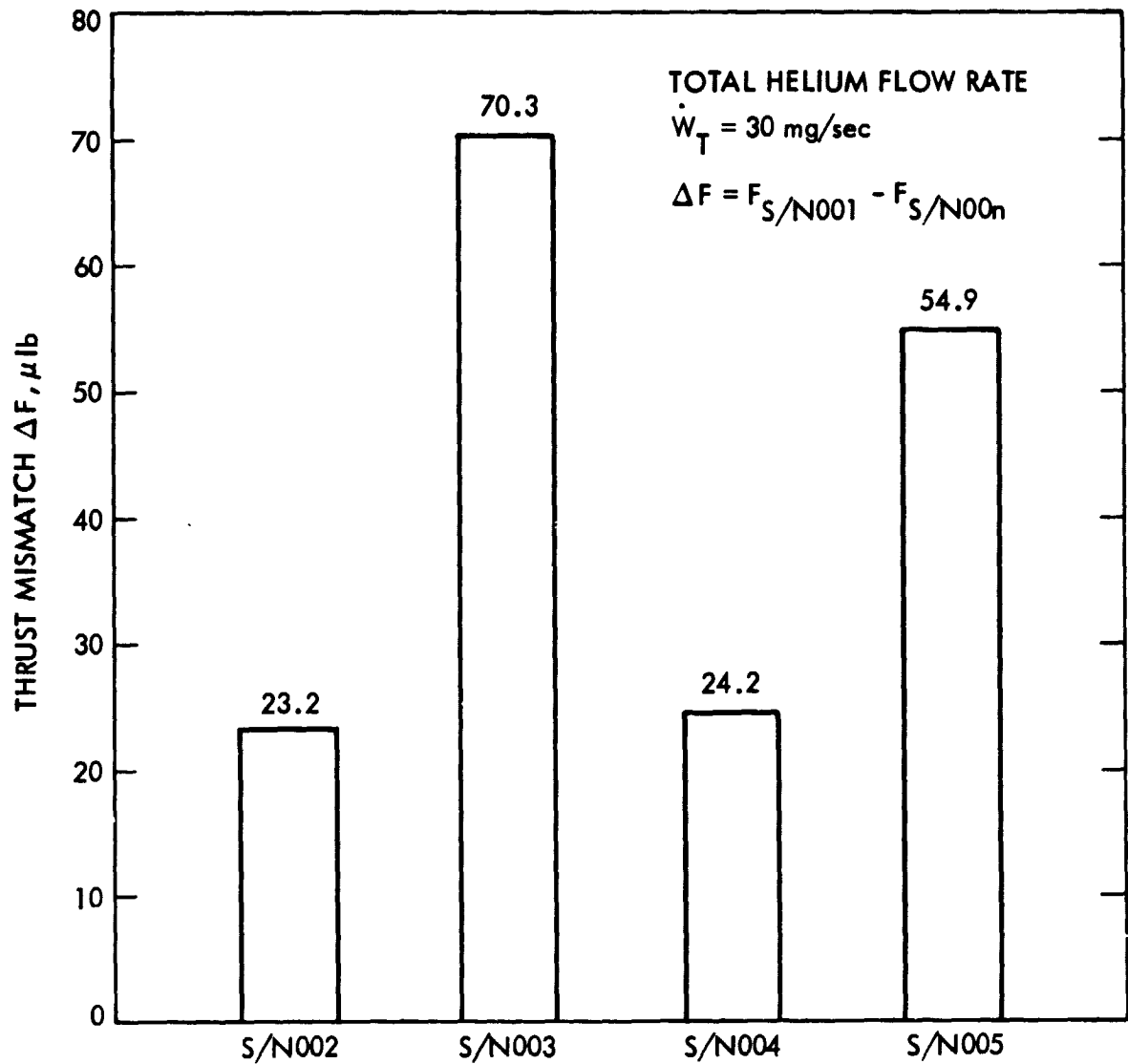


Figure 15 Measured Thrust Mismatch Between Nozzle S/N001 and
Nozzles S/N002 through S/N005

ORIGINAL PAGE IS
OF POOR QUALITY

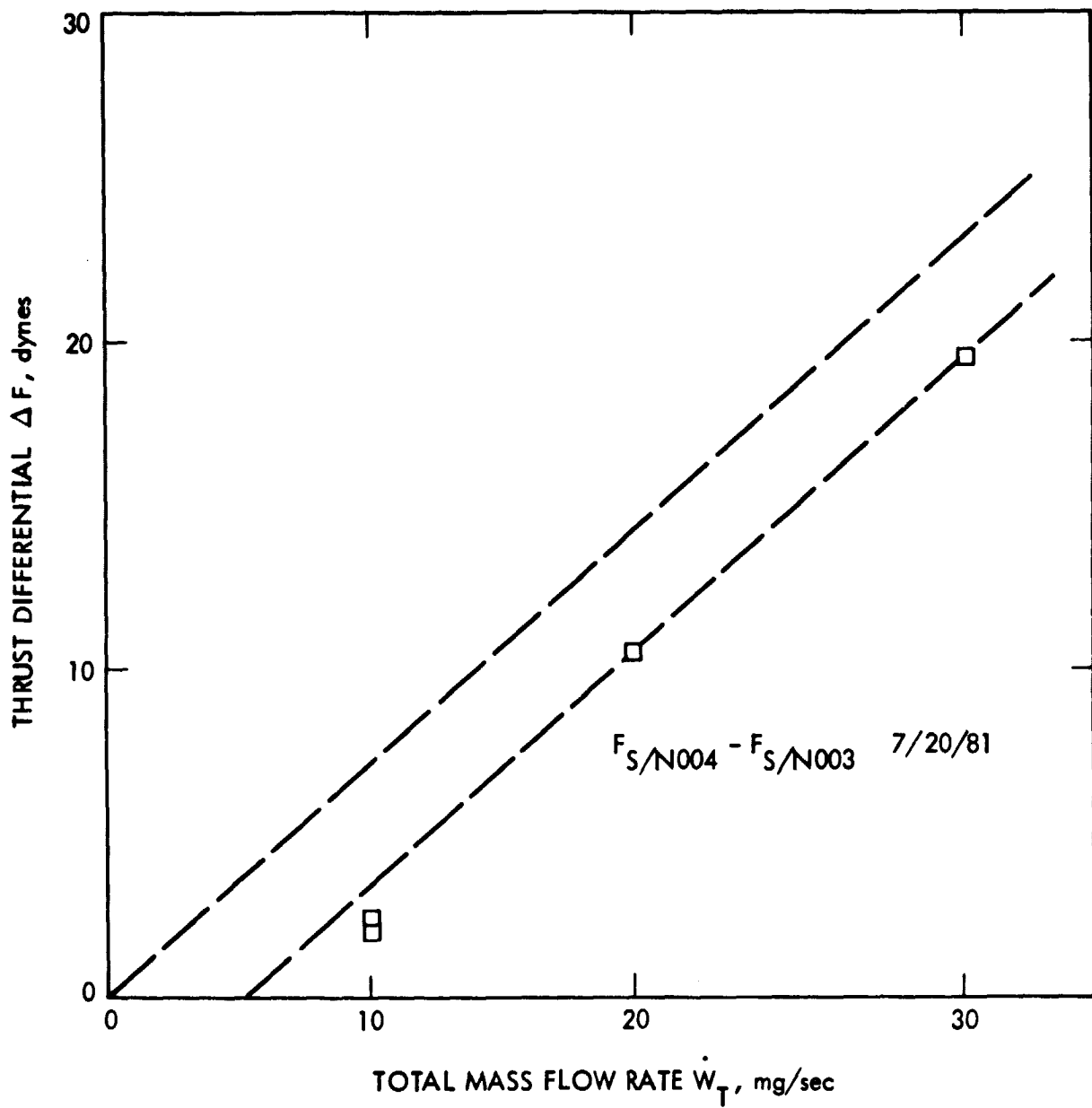


Figure 16 Indicated Thrust Mismatch Between Nozzles
S/N004 and S/N003

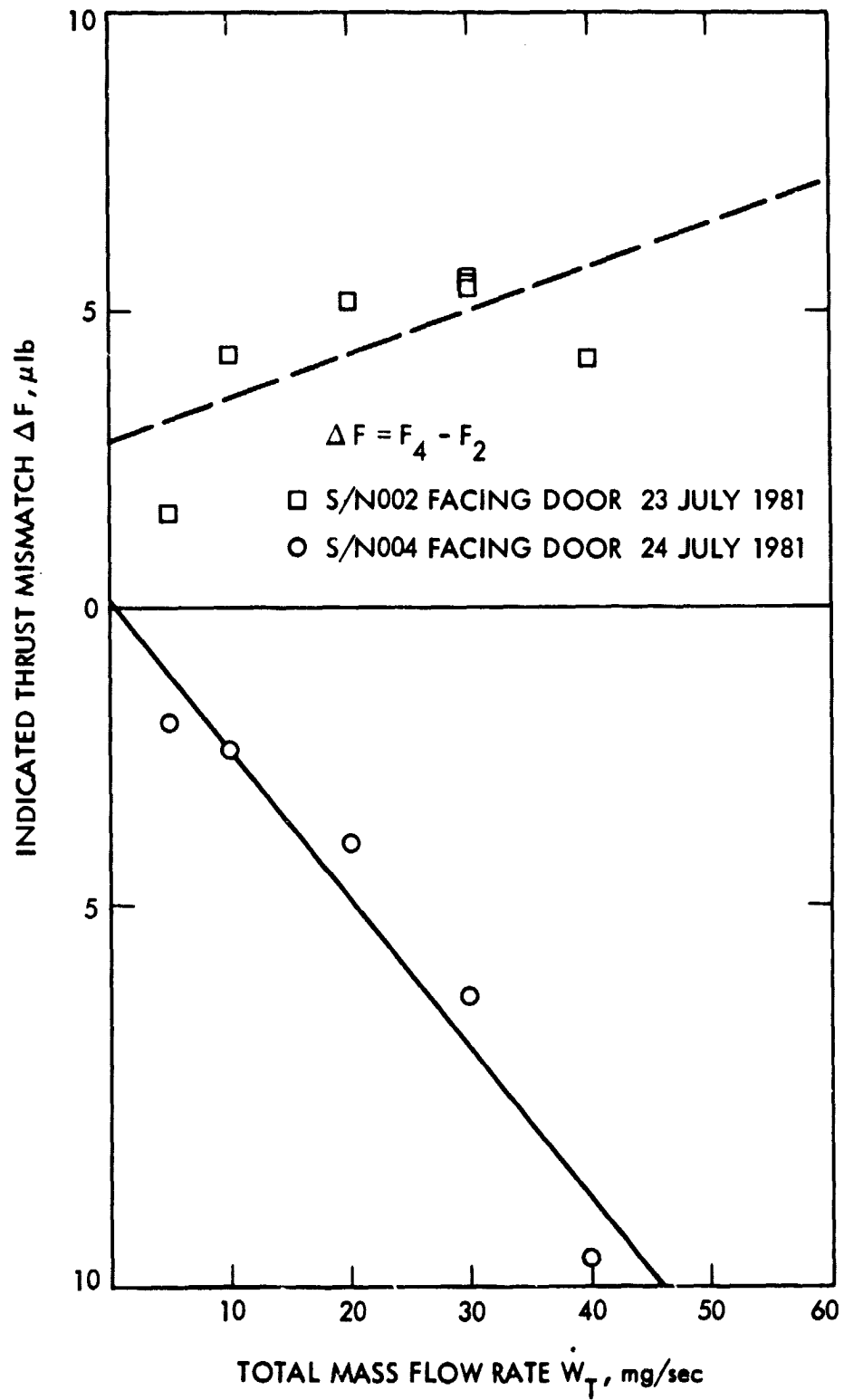


Figure 17 Effect of Torque Direction on Indicated Torque

3.4 Estimate of Angular Deviation of Thrust Vector

In the description of the MERTS thrust measuring stand it was shown that the device does not measure a thrust but a torque from which the thrust is deduced by assuming that the direction of the thrust vector is known and equal to the vector of the applied force used in calibrating the thrust stand. Conversely, it is possible to determine the direction of the thrust vector in the torque plane by measuring the torque when the magnitude of the thrust vector is known. Since the angular deviation of the thrust vector from the y-axis has been shown to be a major parameter affecting the stability of the spacecraft (Figures 5 through 7), an attempt was made to deduce this value from the theoretical thrust and the measured torque, thereby bracketing the angular thrust vector deviation of the selected two nozzles, S/N002 and S/N004.

From the derivation of the torque relation for the thrust measuring stand as presented in Appendix B, the torque due to two nozzles mounted opposite to each other is given by

$$T = F_1 \cos \theta_1 [(L - h_1 \sin \alpha) \cos(\alpha + \theta_1) - h_1 \sin(\alpha + \theta) \cos \alpha] \\ - F_2 \cos \theta_2 [(L + h_2 \sin \alpha) \cos(\alpha + \theta_2) + h_2 \sin(\alpha + \theta_2) \cos \alpha] \quad (24)$$

where	θ_n	inclination of the thrust vector with respect to the torque plane, degree
	θ_n	inclination of the thrust vector with respect to the manifold axis in the torque plane, degree
	α	inclination of the manifold, degree
	L	torque arm, cm
	h_n	manifold length, cm

In the test setup the torque arm L and the manifold lengths h_1 and h_2 were

$$L = 50 \text{ cm}$$

$$h_1 = h_2 = 30 \text{ cm}$$

The theoretical thrust of nozzle n is given by

$$F_n = ((C_f \dot{W}_T) / (m_1 + m_2)) m_n \quad (25)$$

To evaluate an upper bound of the angular misalignment it can be assumed that all effects on the torque due to the

ORIGINAL PAGE IS
OF POOR QUALITY

misalignment of the individual thrust vectors can be attributed to the misalignment of only one of the two nozzles with respect to the other nozzle which is fully aligned, i.e.,

$$\theta_2 = 0.0$$

$$\theta_2 = 0.0$$

Furthermore it will be assumed that the manifold was mounted on the thrust stand without angular misalignment, i.e.,

$$\alpha = 0.0$$

For these conditions the torque relation 25 reduces to

$$T/L = F_1 \cos \theta_1 [\cos \theta_1 - (h_1/L) \sin \theta_1] - F_2 \quad (26)$$

For nozzles S/N002 and S/N004 the factors m_n are from Table 4

$$m_2 = 0.20825 \text{ mg/torr}$$

$$m_4 = 0.20734 \text{ mg/torr}$$

and the thrust factor C_f is

$$C_f = 154.48 \text{ dynes/(mg/sec)}$$

At a total flow rate of $\dot{W}_T = 30 \text{ mg/sec}$ the most likely apparent torque on the thrust stand resulting from the thrust vectors of the two nozzles was

$$T = 4.4481xL \text{ dyn-cm}$$

The magnitude of the two thrust vectors can be evaluated from the flow rate measurements to have been

$$F_2 = 2,322.27 \text{ dynes}$$

and

$$F_4 = 2,312.13 \text{ dynes}$$

so that the actual thrust mismatch could have been

$$\Delta F_{2-4} = 10.15 \text{ dynes}$$

This absolute thrust difference could not have been established by testing the nozzle pair on the thrust stand as only a torque can be measured with this device. The most likely combinations of angular misalignment that could have produced the measured torque with the probable thrust vectors can be ascertained from

$$\theta_1 = \cos^{-1} \{ [(\Delta T/L) + F_2] / F_1 [\cos \theta_1 - (h_1/L) \sin \theta_1] \} \quad (27)$$

The maximum angle $\theta_{1\max}$ could have occurred when

$$\theta_1 = 0.0$$

or

$$\cos \theta_1 = 1$$

$$\theta = \cos^{-1} 1$$

By setting the value in the bracket equal to 1

$$\theta_{1\max} = \delta - \sin^{-1} \{ [(\Delta T/L) + F_2] \sin \delta / F_1 \} \quad (28)$$

where

$$\delta = \tan^{-1} 1 / (h/L) \quad (29)$$

All possible combinations of the two angles θ_1 and θ_2 of the thrust vector are presented graphically in Figure 18. The most likely combination would be for the two angles to be approximately equal. It would then be estimated that

$$\theta_1 = \theta_2 = 0.75 \text{ degree}$$

This conclusion is based on the following consideration. When angle θ reaches its maximum $\theta_{\max} = 0.7506$ degree, angle $\theta_1 = 0.0$, which is most unlikely. When the angle θ_1 is less than $\theta_1 = 0.75$ degree, angle θ_2 has to be much larger than angle θ_1 , which again is not likely to occur. Therefore, it would be most probable for the two angles θ and θ to have been approximately equal. Since the calculated angles are actually the sum of two angles, i.e.,

$$\theta = \theta_1 + \theta_2$$

$$\theta = \theta_1 + \theta_2$$

each nozzle can be charged with one half of the apparent misalignment angle, i.e.,

$$\theta_2 = \theta_4 = 0.375 \text{ degree}$$

$$\theta_2 = \theta_4 = 0.375 \text{ degree}$$

This value is slightly higher than the allowable value

$$\theta = 0.343 \text{ degree}$$

for maintaining stability around the y-axis as shown in Figure 6.

ORIGINAL PAGE IS
OF POOR QUALITY

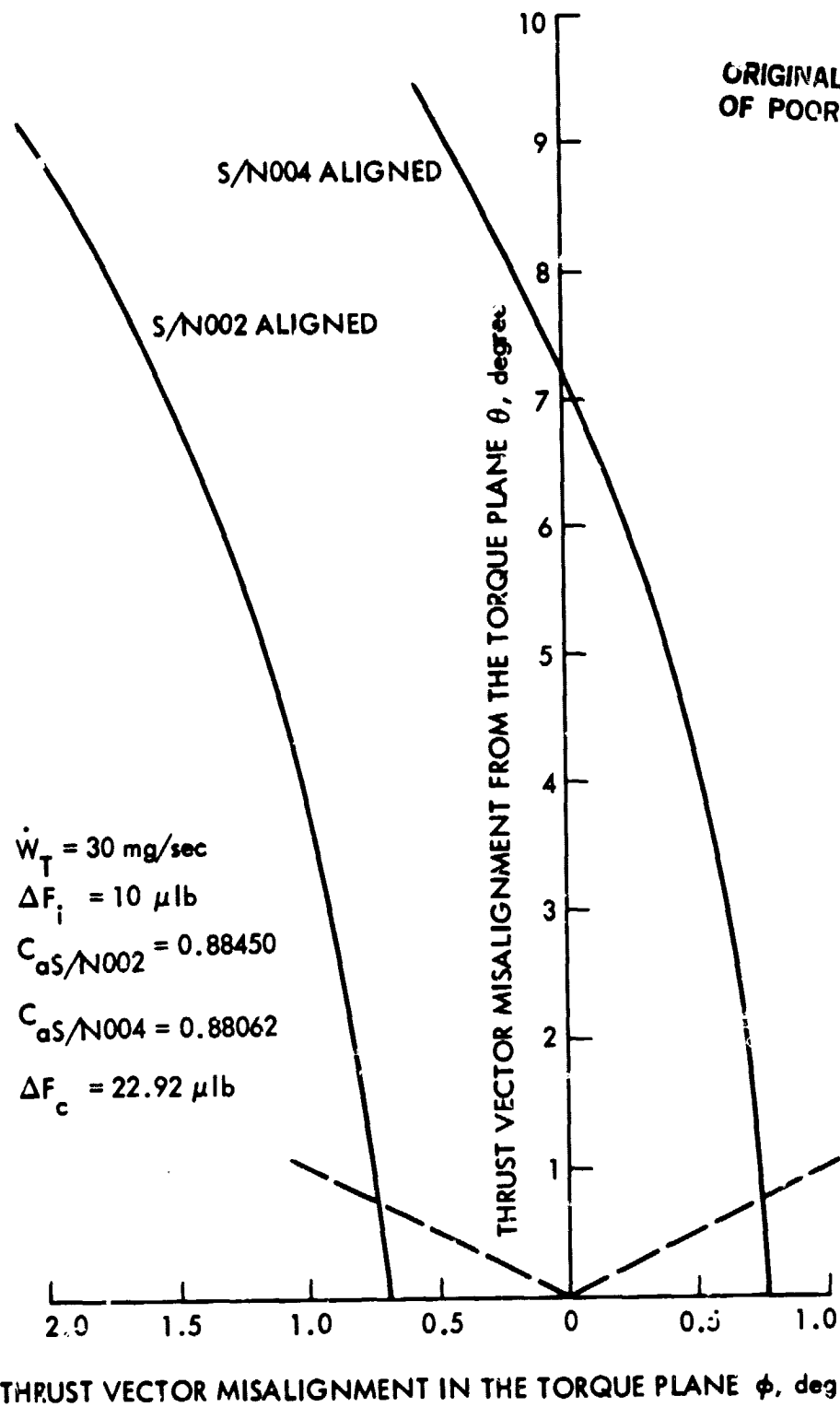


Figure 18 Possible Angular Thrust Vector Misalignment
Combinations for the Measured Torque with Nozzle
Pair S/N002 and S/N004

SECTION 4

CONCLUSIONS

The analysis of the ACT nozzles indicated rather severe restraints on the allowable mismatch between the two thrust vectors with respect to their absolute magnitude and their angular misalignment. For a torque correction capacity $T_c = 5 \times 10^3$ dyn-cm and a total vent flow rate $\dot{W}_T = 30$ mg/sec, the maximum deviation of the thrust vector could not be larger than $\Delta F = 14.4$ dynes or no more than 0.6 percent of the nominal thrust. The angular misalignment of the thrust vector had to be restricted to 0.34 degree.

The various test data which were generated by flow and torque measurements permitted the selection of two nozzles whose thrust differed by less than the allowable maximum value. An estimate of the most likely thrust vector misalignment which was based on the flow tests as well as on the thrust stand data of nozzles S/N002 and S/N004 indicated a probable angular misalignment slightly higher than the permissible value, i.e., 0.375 degree vs. 0.34 degree.

Since the upper bounds of the torque correction capacity were based on the assumption of some degradation of the actual design torque capacity of the attitude control system and since furthermore the thrusts resulting from the venting of helium were based on the upper limits of the venting flow rate, the probability of destabilizing the IRAS spacecraft by activating the ACT Low Thrust Venting System appeared to be very low.

The selection of the two vent nozzles and their mounting proved to satisfy all the requirements for safe venting of helium within the capability of the attitude control system. The spacecraft has been performing under full control of its attitude control system during the entire time when cooling of the ACT was required.

REFERENCES

1. R. F. Cuffel, Computer Program Description For Laminar Nozzle Flow Prediction and Global Plume Backflow Estimate, May 1975 (Private Communication L. Back, JPL)

APPENDIX A

CONVERSION OF SPHERICAL COORDINATE ANGLES
TO
CLOCK AND CONE ANGLES

The ideal nozzle axis is along the y-axis of the spherical coordinate system. The angular inclination of the thrust vector to the y-axis is considered the cone angle α . The vector when projected onto the x-z plane has a clockwise angular displacement from the positive z-axis which is considered the clock angle β .

In the spherical coordinate system the thrust vector has an angular displacement with respect to the x-y plane equal to the angle θ . When the vector is projected onto the x-y plane it has an angular displacement with respect to the positive x-axis equal to the angle ϕ .

The y-component of the unit vector can be expressed in the two coordinate systems by

$$y = \sin\theta\cos\phi \quad (A-1a)$$

$$y = \cos\alpha \quad (A-1b)$$

The z-component of the unit vector can be expressed in the two coordinate systems by

$$z = \sin\alpha\cos\beta \quad (A-2a)$$

$$z = \sin\theta \quad (A-2b)$$

By equating relations A-1a with A-1b and relations A-2a with A-2b

$$\cos\alpha = \sin\theta\cos\phi \quad (A-3)$$

$$\sin\alpha\cos\beta = \sin\theta \quad (A-4)$$

When solving relations A-3 and A-4 for the cone angle α and the clock angle β the two transfer relations for the two coordinate systems are found.

$$\alpha = \cos^{-1}(\sin\theta\cos\phi) \quad (A-5)$$

$$\beta = \cos^{-1}\{\sin\theta/(1 - \sin^2\theta\cos^2\phi)^{1/2}\} \quad (A-6)$$

APPENDIX B

MERTS THRUST MEASURING DEVICE PRINCIPLE

For the evaluation of the observed displacement of the thrust balance during testing of the ACT nozzles the relationship of the major parameters affecting the indicated thrust have to be determined. The geometrical values that influence the output of the thrust measuring device are shown in Figure B-1.

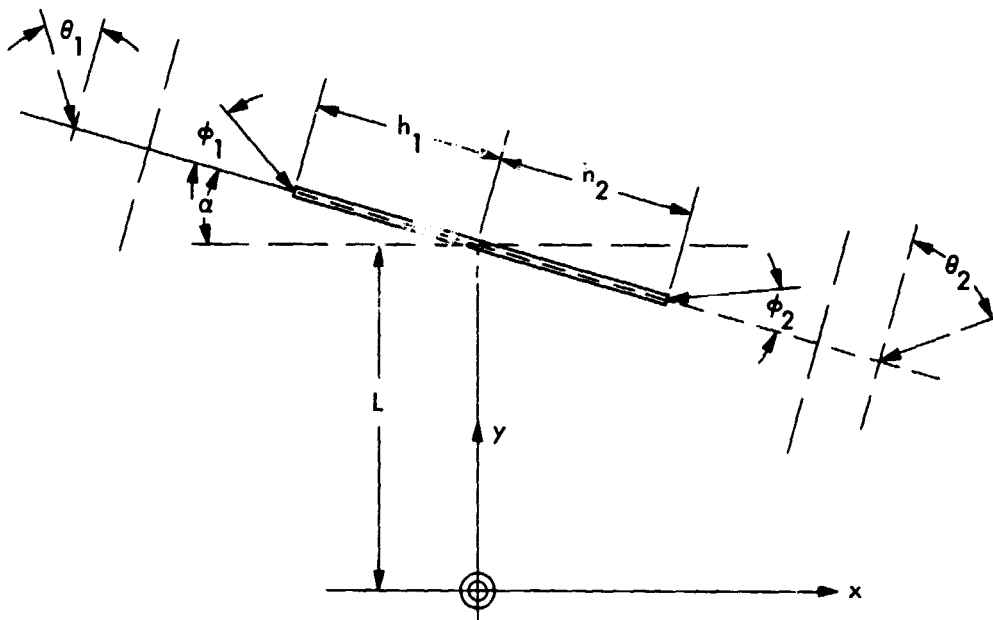


Figure B-1 Geometrical Parameters of the MERTS Thrust Balance

The thrust components of the two nozzles along the x-axis are

$$F_{x1} = F_1 \cos \theta_1 \cos(\alpha + \theta_1) \quad (B-1)$$

$$F_{x2} = F_2 \cos \theta_2 \cos(\alpha + \theta_2) \quad (B-2)$$

The thrust components of the two nozzles along the y-axis are

$$F_{y1} = F_1 \cos \theta_1 \sin(\alpha + \theta_1) \quad (B-3)$$

$$F_{y2} = F_2 \cos \theta_2 \sin(\alpha + \theta_2) \quad (B-4)$$

The total torque imposed upon the thrust device by the exhaust of the total vent flow through the two nozzles is therefore

$$T = F_1 \cos \theta_1 [(L - h_1 \sin \alpha) \cos(\alpha + \theta_1) - h_1 \sin(\alpha + \theta_1) \cos \alpha] \\ - F_2 \cos \theta_2 [(L + h_2 \sin \alpha) \cos(\alpha + \theta_2) + h_2 \sin(\alpha + \theta_2) \cos \alpha] \quad (B-5)$$